MARTIN MARIETTA ENERGY SYSTEMS LIBRARIES
3 4456 0361496 1

CENTRAL RESEARCH LIBRARY
DOCUMENT COLLECTION

5

ORNL-2946
UC-25 - Metallurgy and Ceramics

THE STABILITY OF EUROPIUM OXIDE IN SILICON-BEARING STAINLESS STEEL

C. F. Leitten, Jr.

CENTRAL RESEARCH LIBRARY
DOCUMENT COLLECTION
LIBRARY LOAN COPY
DO NOT TRANSFER TO ANOTHER PERSON
If you wish someone else to see this document, send in name with document and the library will arrange a loan.

OAK RIDGE NATIONAL LABORATORY
operated by
UNION CARBIDE CORPORATION
for the
U.S. ATOMIC ENERGY COMMISSION

Printed in USA. Price $2.25. Available from the

Office of Technical Services
Department of Commerce
Washington 25, D.C.

LEGAL NOTICE

This report was prepared as an account of Government sponsored work. Neither the United States, nor the Commission, nor any person acting on behalf of the Commission:

A. Makes any warranty or representation, expressed or implied, with respect to the accuracy, completeness, or usefulness of the information contained in this report, or that the use of any information, apparatus, method, or process disclosed in this report may not infringe privately owned rights; or

B. Assumes any liabilities with respect to the use of, or for damages resulting from the use of any information, apparatus, method, or process disclosed in this report.

As used in the above, "person acting on behalf of the Commission" includes any employee or contractor of the Commission, or employee of such contractor, to the extent that such employee or contractor of the Commission, or employee of such contractor prepares, disseminates, or provides access to, any information pursuant to his employment or contract with the Commission, or his employment with such contractor.

ORNL-2946

Contract No. W-7405-eng-26

METALLURGY DIVISION

THE STABILITY OF EUROPIUM OXIDE IN SILICON-BEARING STAINLESS STEEL

C. F. Leitten, Jr.

DATE ISSUED

AUG 9 1960

Submitted as a thesis to the Graduate Council of The University of Tennessee in partial fulfillment of the requirements for the degree Master of Science

OAK RIDGE NATIONAL LABORATORY
Oak Ridge, Tennessee
operated by
UNION CARBIDE CORPORATION
for the
U.S. ATOMIC ENERGY COMMISSION

MARTIN MARIETTA ENERGY SYSTEMS LIBRARIES

3 4456 0361496 1

ACKNOWLEDGMENT

The author is indebted to Dr. E. E. Stansbury for his guidance and encouragement throughout the course of this investigation and for his corrective criticisms which led to the preparation of the final manuscript.

Realizing the impossibility of acknowledging everyone who contributed to the accomplishment of this work, the author wishes to extend special thanks to the following members of the Oak Ridge National Laboratory staff: R. J. Beaver for his assistance and cooperation in implementing the investigation; J. H. Coobs, H. L. Yakel, Jr., D. E. LaValle, P. F. Thomason, and W. R. Laing for their direct contributions and helpful discussions during the investigation; and J. E. Cunningham whose advice and assistance in the preparation of the final manuscript are greatly appreciated.

Direct assistance in accumulating the experimental data for this study was provided by the following Oak Ridge National Laboratory personnel: L. Queener, melting and casting of the experimental alloys; E. R. Turnbill, J. W. Geer, and J. N. Hix, material preparation, compact fabrication and heat treatment; C. K. H. DuBose, optical microscopy; R. M. Steele, x-ray diffraction; G. Hallerman, reaction product extraction; and H. Kubota, G. Goldberg, G. A. Westerdahl, and S. H. McCarley, chemical analyses. Their contributions are gratefully appreciated.

The author is indebted to Mrs. Louie Mae Pyatt of the Metallurgy Reports Office for her cooperation in typing this manuscript and to

Mrs. Meredith R. Hill for her assistance and cooperation in expediting the preparation of this manuscript.

Appreciation is also extended to the Union Carbide Nuclear Company for its employee educational assistance program.

TABLE OF CONTENTS

CHAPTER		PAGE
I.	SUMMARY	1
II.	INTRODUCTION	4
III.	OBJECTIVES	7
IV.	SURVEY OF PRIOR WORK	8
V.	EXPERIMENTAL PROCEDURES AND EQUIPMENT	12
	Selection and Conditioning of the Eu_2O_3	12
	Selection of the Matrix Materials	18
	Preparation of Powder Metallurgy Test Compacts	18
	Powder Compact Heat Treatment and Volume Change Measurements	22
	Reaction Product Identification	24
VI.	RESULTS AND DISCUSSION	27
VII.	CONCLUSIONS	81
LIST OF REFERENCES		83

LIST OF TABLES

TABLE		PAGE
I.	Quantitative Spectrographic Analyses on the Impurities in Eu_2O_3	13
II.	Type Designation and Corresponding Conditioning Variables for the Eu_2O_3	17
III.	Chemical Composition of the Prealloyed Stainless Steel Dispersants Employed in the Compatibility Tests	19
IV.	Chemical Composition of the Various Elemental Dispersants	20
V.	Silicon Content of the Dispersant Materials	21
VI.	Effect of Silicon on the Stability of Eu_2O_3 in Various Matrix Materials	28
VII.	Spectrographic Analysis of H_2O Removed from Surface of a Reacted Eu_2O_3-Type 304B Stainless Steel Compact	36
VIII.	Effect of Oxide Conditioning on Stability of Eu_2O_3 in Various Dispersants Heat Treated at 1230°C under Hydrogen	43
IX.	Effect of Oxide Conditioning on Stability of Eu_2O_3 in Various Dispersants Heat Treated at 1230°C under Helium	45
X.	Effect of Temperature and Time on the Compatibility of Eu_2O_3 in Various Dispersants	60
XI.	Effects of Heat Treatment on Eu_2O_3-Bearing Silicon and Eu_2O_3-Bearing SiO_2 Dispersions	66

TABLE PAGE

XII. Summary of Results on Various Cast Europium-Silicon Alloys 69

XIII. Spectrographic Analysis on Reaction Product Films Extracted from Different Specimens 76

XIV. The Oxygen Content of Heat Treated 30 Weight Per Cent Type D-Eu_2O_3-347B Stainless Steel Compacts as a Function of Heating Time and Atmosphere 78

LIST OF FIGURES

FIGURE PAGE

1. Furnace assembly for high firing the lanthanon oxides 15
2. Microstructure of a 30 weight per cent type D-Eu_2O_3 dispersion in type 304B stainless steel heat treated at 1230°C for one and one-half hours under hydrogen. As polished. 500X 32
3. Same as Figure 2 except for being exposed to demineralized-distilled water. As polished. 500X 33
4. Microstructure of a 30 weight per cent type D-Eu_2O_3 dispersion in type 347B stainless steel heat treated at 1230°C for one and one-half hours under hydrogen. As polished. 500X 34
5. Microstructure of a 30 weight per cent type D-Eu_2O_3-nickel compact heat treated at 1230°C for one and one-half hours under hydrogen. As polished. 500X 37
6. Microstructure of a 30 weight per cent type D-Eu_2O_3 dispersion in type I-chromium heat treated at 1230°C for one and one-half hours under hydrogen. As polished. 1000X 38
7. Microstructure of a 30 weight per cent type D-Eu_2O_3 dispersion in type III-chromium heat treated at 1230°C for one and one-half hours under hydrogen. As polished. 1000X 39

FIGURE PAGE

8. Microstructure of a 30 weight per cent type D-Eu_2O_3 dispersion in type II-chromium heat treated at 1230°C for one and one-half hours under hydrogen. As polished. 1000X 41

9. Microstructure of a 30 weight per cent type D-Eu_2O_3-type 304B stainless steel compact heat treated at 1230°C for one and one-half hours under helium. As polished. 1000X 48

10. Microstructure of a 30 weight per cent type D-Eu_2O_3 dispersed in type 347B stainless steel and heat treated at 1230°C for one and one-half hours under helium. As polished. 1000X 49

11. Microstructure of a 30 weight per cent type B-Eu_2O_3-304B stainless steel dispersion heat treated at 1230°C for one and one-half hours under helium. As polished. 1000X . . 50

12. Microstructure of 30 weight per cent type B-Eu_2O_3 dispersed in type 347 stainless steel and heat treated at 1230°C for one and one-half hours under helium. As polished. 1000X 51

13. Microstructure of 30 weight per cent type E-Eu_2O_3 dispersed in nickel and heat treated at 1230°C for one and one-half hours under hydrogen. As polished. 1000X . 53

14. Microstructure of 30 weight per cent type B-Eu_2O_3 dispersed in nickel and heat treated at 1230°C for one and one-half hours under hydrogen. As polished. 1000X . 54

FIGURE PAGE

15. Microstructure of 30 weight per cent type C-Eu_2O_3 dispersed in nickel and heat treated at 1230°C for one and one-half hours under hydrogen. As polished. 500X . 55

16. Microstructure of 30 weight per cent type D-Eu_2O_3 dispersed in nickel and heat treated for one and one-half hours at 1230°C under helium. As polished. 1000X . 56

17. Microstructure of 30 weight per cent type D-Eu_2O_3 dispersed in type 304L stainless steel and heat treated at 1230°C for one and one-half hours under hydrogen. As polished. 1000X 57

18. Microstructure of a 30 weight per cent type D-Eu_2O_3 dispersion in type 304L stainless steel heat treated at 1230°C for one and one-half hours under helium. As polished. 1000X 58

19. Microstructure of a 30 weight per cent type D-Eu_2O_3 dispersion in type 347B stainless steel heat treated at 1230°C for 16 hours under hydrogen. As polished. 500X . 63

20. Microstructure of 30 weight per cent type D-Eu_2O_3 dispersed in type 304L stainless steel and heat treated 16 hours at 1230°C under hydrogen. As polished. 1000X . 64

21. Microstructure of 30 volume per cent type D-Eu_2O_3 dispersed in silicon and heat treated at 1200°C for one and one-half hours under hydrogen. As polished. 500X . 68

FIGURE PAGE

22. Microstructure of the cast 22.4 weight per cent europium-silicon alloy under (a) bright field and (b) polarized light. As polished. 500X 71

23. Microstructure of the cast 73.7 weight per cent europium-silicon alloy under (a) bright field and (b) polarized light. As polished. 500X 72

24. Microstructure of the cast 84.88 weight per cent europium-silicon alloy under (a) bright field and (b) polarized light. As polished. 500X 73

CHAPTER I

SUMMARY

The stability of Eu_2O_3 dispersed in silicon-bearing stainless steel powder compacts was studied in the temperature range 900–1250°C. The effects of silicon content of the stainless steel powder, oxide conditioning treatment, and heat-treating time and atmosphere were also investigated.

Independent of the conditioning process employed, Eu_2O_3 reacted with the austenitic stainless steel as manifested by compact volume increases and the deposition of an europium-bearing, yellow-green film on the specimen surfaces. The degree of reaction was observed to increase with increasing silicon content in the steel. Volume increases of approximately six per cent were noted in stainless steel-base compacts containing two weight per cent silicon when heat treated at 1230°C for one and one-half hours. The presence of a reaction product was also observed in the Eu_2O_3 particles in the high silicon-bearing stainless steel compacts as a result of reaction. Stainless steel-base dispersions containing 0.11 weight per cent silicon possessed slight volume decreases on heat treating; however, the deposition of the reaction film was also noted on these specimen surfaces. The presence of a reaction product in the oxide particles was not observed in these compacts.

Elemental iron, nickel, and chromium with silicon content less than 58 parts per million were stable with Eu_2O_3 at a temperature of 1230°C. Depending on the oxygen content of the chromium,

slight interactions of Eu_2O_3 and chromium oxide were noted at the particle interfaces. The instability noted between Eu_2O_3 and chromium containing 0.12 weight per cent silicon was manifested by a volume increase and the deposition of the yellow-green reaction film. No reaction product, however, was noted in the europium oxide particles.

The heat-treating atmosphere did not appear to affect the presence of the reaction in the investigated material combinations but did affect the degree of reaction. Specimens heat treated in hydrogen appeared to have larger volume growths than compacts heat treated in helium or vacuum. Independent of the atmosphere, the degree of reaction was observed to increase with time and temperature.

Efforts to establish basic standards for identification of the various reaction products involved studies on the europium-silicon alloy system and on Eu_2O_3 dispersions in silicon and SiO_2. The reaction of Eu_2O_3 with silicon and with SiO_2 at 1200°C generally resulted in compact volume increases and the deposition of the yellow-green film on the specimen surfaces. The formation of $EuSi_2$ was positively established as a reaction product in the silicon-base compacts. Few difficulties were encountered in preparing the various europium-silicon alloys by arc melting other than a considerable loss of europium which was noted in each alloy as a result of vaporization. A preliminary study was made on these alloys in the composition range 9–91 per cent europium. The possible existence of at least three silicides was noted by examination of x-ray diffraction patterns. The cast microstructure of alloys between 9 and 63 weight per cent europium consisted of silicon and $EuSi_2$.

Because of difficulties encountered in isolating and identifying the various reaction products, only a postulated reaction mechanism is presented in this report. More definitive conclusions regarding the reaction products and mechanisms could not be realized due to a lack of fundamental physical and chemical information on europium and its compounds.

CHAPTER II

INTRODUCTION

Considerable effort has been expended in the Army Package Power Program at the Oak Ridge National Laboratory in developing a suitable neutron-absorbing materials combination for control of the Stationary Medium Power Reactor (SM-1) presently operating at Fort Belvoir, Virginia. In general, the recent absorber program has centered on the development of stainless steel roll-clad composite plates containing lanthanon oxide-bearing dispersions. These dispersions have been considered since it became evident that an improved absorber material with greater burnup capability would be required for future operation of the SM-1. The initial Core I absorber consisted of composite plates containing three weight per cent enriched boron-10 dispersed in electrolytic iron as core material and clad with stainless steel. Boron-10 undergoes an n,α reaction during exposure to neutron bombardment with the result that boron-bearing bodies may develop dimensional instability by swelling due to the attendant generation of helium. For example, miniature stainless steel-clad absorber samples of SM-1 using Core I design exhibited core-clad separation and swelling after 15 per cent burnup of the boron-10 atoms during irradiation testing in the Materials Test Reactor (MTR). Similar type separations and swelling were noted at the tip ends of the Core I boron-iron absorber sections after ten megawatt year neutron exposure in the SM-1.

Unlike boron-10, the high neutron-absorbing lanthanons do not yield gaseous products such as helium under irradiation and thus the

damage due to the evolution and expansion of gas with temperature would not be encountered. Hence, a program was initiated to investigate the potential of europium in the form of Eu_2O_3 as a likely alternate for boron. Europium was selected over the other high neutron-absorbing lanthanons chiefly because of its superior burnout characteristics. The europium (n,γ) reaction yields a series of four europium isotopes all of which possess comparatively high neutron-capture sections in the energy ranges of interest. Although final emphasis was placed on Eu_2O_3-bearing compacts because of nuclear properties, considerable development work was done initially using various lanthanon oxide mixtures. These mixtures were investigated as a substitute for Eu_2O_3 since they were relatively cheap and it appeared reasonable that the mixtures should possess similar chemical characteristics. These materials as obtained from the various vendors were of low density and strength and of extremely fine particle size. The oxides were thus conditioned by high-temperature firing to produce desirable physical and chemical characteristics.

Prior to the consolidation and fabrication studies, the compatibility of the lanthanon oxide mixtures with type 304B stainless steel was studied. This study was conducted since experience has shown that, although various material combinations appeared stable under standard conditions, severe compatibility problems existed under actual processing conditions. The initial compatibility tests between the lanthanon oxide mixtures and type 304B stainless steel showed that this materials combination was stable at temperatures up to 1250°C. Procedures were thus developed for conditioning the received oxide mixtures,

preparing homogeneous powder metallurgy dispersions, and fabricating roll-clad composite-type plates (1). Employing these established procedures, powder metallurgy dispersions of Eu_2O_3 were then prepared. Unlike the lanthanon oxide mixtures, Eu_2O_3 was not stable in type 304B stainless steel when sintered in a hydrogen atmosphere at 1230°C for one and one-fourth hours. The reaction was manifested by a compact volume increase and the evolution of a compact constituent which coated the entire surface of the compact. Survey compatibility studies of Eu_2O_3 with various types of stainless steel and with the basic stainless steel constituents indicated that the possible cause of the instability was related to the silicon content of the matrix material. Fortunately, as a result of this observation acceptable dispersions of Eu_2O_3 in stainless steel were prepared and subsequently absorber sections were manufactured for Core II of the SM-1.

The successful manufacture of the Eu_2O_3-bearing absorbers, however, did not resolve the startling dissimilarity between the compatibility of Eu_2O_3 and the lanthanon oxide mixtures in the silicon-bearing stainless steels. It was, therefore, the purpose of the study presented herein to determine the effect of silicon on the stability of Eu_2O_3 in stainless steel and postulate a mechanism by which silicon enters into the reaction.

CHAPTER III

OBJECTIVES

The basic objectives of this study were to determine the effect of silicon on the stability of Eu_2O_3 in stainless steel and postulate a mechanism by which silicon enters into the reaction. The effect of silicon on the compatibility of Eu_2O_3 with stainless steel was evaluated by heat treating powder specimens. As a result the following factors were selected for evaluation:

1. the heat-treating atmosphere, time, and temperature,
2. the type and composition of the matrix material, and
3. the conditioning treatment of the Eu_2O_3.

CHAPTER IV

SURVEY OF PRIOR WORK

Very limited and, in general, only qualitative work has been reported on the stability of Eu_2O_3 in silicon-bearing stainless steel. Early exploratory investigations by Ray and Beck (2) indicated that Eu_2O_3 could be readily incorporated in stainless steel by utilizing powder metallurgy procedures. Dispersion-type specimens were prepared by hot extruding at 1000°C stainless steel cans containing cold-pressed powders. No indication of a reaction between the lanthanon oxide and stainless steel was noted in any of the extrusions. However, examination of unclad compacts containing 20 and 30 weight per cent Eu_2O_3 in stainless steel which were irradiated for two cycles in the MTR revealed a significant decrease in ductility, structural damage adjacent to the Eu_2O_3 particles, and slight volume increase (3). Similar type specimens containing Gd_2O_3 dispersed in stainless steel and irradiated two cycles in the MTR showed only a slight decrease in ductility with no structural damage or volume increase. Later it was demonstrated by Leitten (1) that Eu_2O_3, dispersed in stainless steel with a silicon content greater than 0.03 weight per cent and heat treated at 1230°C for one and one-fourth hours, reacted with the stainless steel and caused severe swelling of the compacts. This observation suggested the possibility that the damage found after the previous irradiation tests was associated with a similar reaction in the specimen as a result of the irradiation temperature. These preliminary observations by Leitten (4) from a limited series of compatibility tests also

permitted the establishment of specifications and subsequently the successful manufacture of stable Eu_2O_3-bearing stainless steel control rods. More recent studies showed that the stability of Eu_2O_3 in Nichrome powder is dependent on silicon content. The reaction observed in the Nichrome-base compacts of silicon content greater than 0.1 per cent was also manifested by a volume increase.

Since the dispersion-type compacts were to be consolidated by a cold-press and sinter powder metallurgy operation, concern arose over the interaction of the lanthanon oxides with various metallic oxides at elevated temperatures. These metallic oxides can easily result if, during the sintering operation, care is not taken to control the hydrogen dew point. Most metallic powders, per se, also contain considerable surface oxide. Investigations were reported on mixtures of several transition elements and lanthanon oxides of the type ABO_3 where "B" represents a trivalent transition element and "A" represents a trivalent lanthanon element. The crystal structure of the orthoferrite crystals of gadolinium, samarium, and europium were investigated by Geller (5). He established by x-ray diffraction that these orthoferrites are orthorhombic with a distorted perovskite structure. An optical examination of the gadolinium, samarium, and europium orthoferrites indicated that by transmitted light the orthoferrites are orange-brown but by reflected light, $GdFeO_3$ is very dark brown with adamantine luster and that $EuFeO_3$ is very dark brown with an adamantine to submetallic luster. The lanthanum-and neodymium-nickel oxides were prepared by Wold, Post, and Banks (6). Similar attempts to prepare the nickel oxides of samarium, gadolinium, and yttrium were not successful

when firing the reactants in air at 800°C. The lanthanon manganites of lanthanum, praseodymium, neodymium, samarium, gadolinium, and yttrium were prepared by Jonker and Van Santen (7) by firing the oxides of the appropriate elements at 1300°C in air. Considerable reaction was also noted in firing the oxide mixtures at 1000°C. The preparation of lanthanon-chromium oxides and lanthanon-cobalt oxides was accomplished by Wold and Ward (8) by heating blended mixtures of the appropriate oxides at 900°C in air. Cerium-, praseodymium-, neodymium-, and samarium-chromium oxides as well as lanthanum-, praseodymium-, neodymium-, and samarium-cobalt oxides were prepared. X-ray examination of the resultant products indicated cubic lattice cells with perovskite structures.

As well as the possible oxide interactions considered above, the direct reduction of Eu_2O_3 or the formation of europium compounds with impurity elements in the hydrogen gas and/or the stainless steel was also postulated. Reduction of Eu_2O_3 could conceivably result in either the formation of the divalent oxide or europium metal. Eick (9) reported that EuO was prepared by the reaction of lanthanum metal with Eu_2O_3 at 1300–1500°C in vacuum. The sublimate which resulted contained EuO and/or europium metal. These europium preparations were found to contain a NaCl-type cubic phase with a lattice parameter of 5.1439 ± 0.0005 Å. A Kjeldahl determination demonstrated that EuN was absent in the diffraction patterns; therefore, Eick assumed that the compound was EuO. In cases where EuN was formed along with EuO a lattice constant a = 5.1328 ± 0.0008 Å was observed. Since this parameter does not correspond to either EuO or EuN which has an a = 5.007 ± 0.004 Å, a

possible partial solubility of EuO in EuN is suggested. Eick also discussed the possible formation of divalent samarium oxide as well as the preparation and crystal structure of $SmO_{0.4-0.6}$.

Since the stability of Eu_2O_3 in austenitic-type stainless steel was initially postulated as being dependent on the silicon content, the possible interaction of silicon and/or of a silicon compound with Eu_2O_3 to yield either a silicide or silicate was suggested. A review of the available literature failed to disclose an europium-silicon equilibrium phase diagram. The preparations of various lanthanon disilicides and determinations of their basic crystal structure were reported by Perri, Binder, and Post (10). Disilicides of cerium, praseodymium, neodymium, samarium, europium, gadolinium, dysprosium, and yttrium were prepared by interacting the appropriate amount of the desired lanthanon oxide with pure silicon. X-ray diffraction studies indicated that cerium, praseodymium, and neodymium disilicides were tetragonal while samarium, gadolinium, dysprosium, and yttrium disilicides were orthorhombic. Unlike the "heavier" lanthanons, $EuSi_2$ was found to crystallize in the tetragonal system with lattice constants a = 4.29 Å and c = 13.66 Å.

No information was available on the formation of the lanthanon silicates. Judging from existing thermodynamic data, the formation of a silicate by reacting SiO_2 with a lanthanon metal appears unlikely. However, the interaction of SiO_2 with the lanthanon oxide, for example Eu_2O_3 or EuO, could result in the formation of a silicate.

CHAPTER V

EXPERIMENTAL PROCEDURES AND EQUIPMENT

During the course of developing the Eu_2O_3-stainless steel dispersion for reactivity control in the SM-1 reactor, it became evident that the physical and/or chemical state of the commercially available oxide needed to be improved. Consequently, a process was developed which consisted of conditioning the Eu_2O_3 at 1700°C for three hours under a hydrogen atmosphere. Since the crystal structure of the Eu_2O_3 changed from body-centered cubic to monoclinic in the course of the high firing, the effect of various degrees of conditioning on the stability of the oxide in stainless steel was considered. Europium oxide was therefore prepared by high firing in air and hydrogen in the temperature range 1500–1900°C.

I. SELECTION AND CONDITIONING OF THE Eu_2O_3

A typical spectrographic analysis of the as-received Eu_2O_3, employed in these studies, is shown in Table I. Experience indicated that for optimum conditioning properties, the initial oxide should be in the as-calcined form, that is, as oxidized from the oxalate at 950–1000°C. This oxide appears "fluffy" in form and closely resembles talcum powder. Since the Eu_2O_3 used in this study was initially extracted from a monozite ore, the oxide was closely inspected for alpha-emitting materials. Any trace of such isotopes was cause for rejection of the starting material.

TABLE I

QUANTITATIVE SPECTROGRAPHIC ANALYSES
ON THE IMPURITIES IN Eu_2O_3

Element	Concentration (wt %)
Al	0.2
Ba	< 0.05
Ca	0.05
Fe	0.03
Si	0.005
Y	0.005
La	0.06
Ce	0.10
Pr	< 0.05
Nd	< 0.05
Sm	< 0.02
Gd	0.005
Yb	0.002

To facilitate handling of the oxide powder, the received material was consolidated into small cylindrical pellets. This operation consisted of pouring approximately 35 grams of the material into the cavity of a double-acting powder metallurgy die, 0.8 inch diameter, leveling, and pressing at a pressure of about four tons per square inch. Normally, a length to diameter ratio equal to one was employed to promote uniform shrinkage during firing. The light pressing pressure was found adequate to prevent surface spallation of the oxide during handling.

The high-temperature heat treatment was accomplished in the induction-type experimental furnace illustrated in Figure 1. As illustrated, the desired number of pellets ranging to a maximum of ten was placed in a tungsten crucible approximately two by two by seven inches in size. Tungsten was selected as the crucible material because of its chemical inertness with the lanthanon oxides in the temperature range 1500–1900°C. Ceramic-type crucible materials Al_2O_3, MgO, and ZrO_2 all reacted with the lanthanon oxides at these elevated temperatures. Upon completion of the loading, the tungsten crucible was inserted in a graphite crucible mounted in the center of an induction coil. Care was exercised in positioning the tungsten crucible to prevent direct contact with the graphite during the subsequent firing. Amorphous, thermatomic carbon powder was packed between the graphite crucible and the outer quartz furnace tube to serve as an insulator. A graphite cover with an attached chimney or sight tube was placed over the graphite susceptor crucible to prevent the thermatomic carbon insulation from contaminating the europium oxide

UNCLASSIFIED
ORNL-LR-DWG 38531

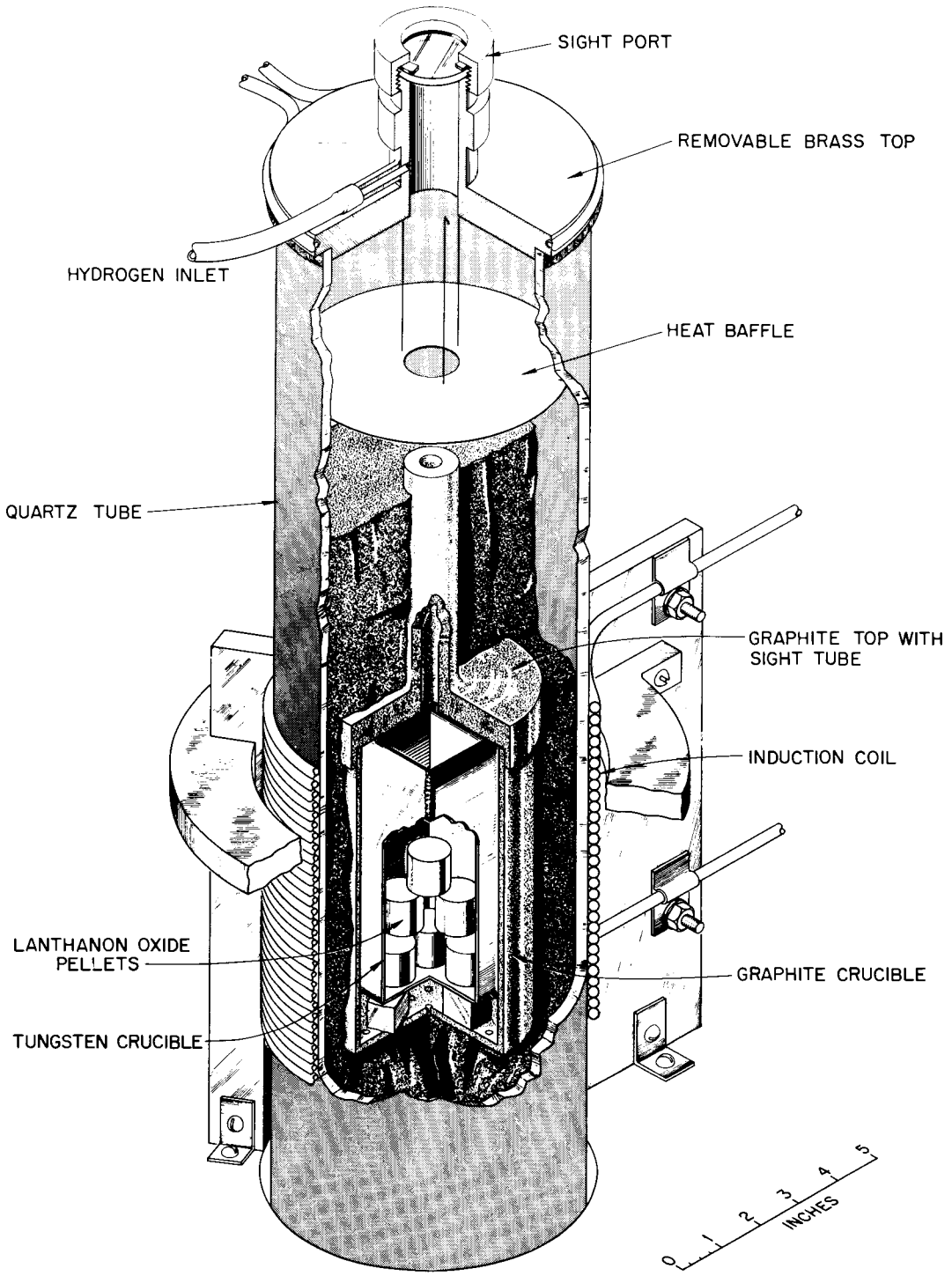

Figure 1. Furnace assembly for high firing the lanthanon oxides.

pellets. The remainder of the quartz tube was then filled with the thermatomic carbon and finally capped with a gastight, brass end plug which was equipped with a sight port and gas inlet stem. When firing was conducted under an atmosphere of hydrogen, a hydrogen gas stem was attached to the lid to permit passage of the gas to the pellets. The exit hydrogen gas escaped through the stem attached to the bottom of the quartz tube. Air firing was conducted similarly, except that the gas inlet stem on the end plug and exit stem on the quartz tube remained open.

The pellet firing was carried out at the desired temperatures for a period of three hours. The power in the converter was varied to control the rate-of-temperature rise in the furnace; normally, a heating rate of 300°C per hour was maintained. Temperature measurements were made on the surface of the top pellet by sighting on optical pyrometer through the end plug sight port. Periodic readings were taken to maintain the pellet surface temperature within 25°C of the intended firing temperature. Upon completion of the firing, the converter was shut off and furnace air cooled to approximately 150°C at which time it was disassembled and the fired pellets removed. When the firing was performed under an atmosphere of hydrogen, care was taken to reduce the water content of the gas by drying. Normally an inlet hydrogen dew point of -62°C as measured by an Alnor Dew Point Meter was maintained.

The conditioned oxide was then crushed to two fraction sizes -325 mesh and -100 +325 mesh with a mortar and pestle and screened frequently throughout the operation to minimize extreme fines. Table II

TABLE II

TYPE DESIGNATION AND CORRESPONDING CONDITIONING VARIABLES FOR THE Eu_2O_3

Oxide Type	Conditioning Variables		
	Temperature (°C)	Time (hr)	Atmosphere
A		As-received	
B	1500	3	H_2
C	1500	3	Air
D	1700	3	H_2
E	1700	3	Air
F	1900	3	H_2
G	1900	3	Air

lists the various types of Eu_2O_3 and their respective conditioning treatments. This identification scheme is followed throughout the remainder of the report.

II. SELECTION OF THE MATRIX MATERIALS

The dispersant materials selected for the compatibility studies were, in general, commercially available. The various grades of prealloyed stainless steel were manufactured by the Vanadium Alloy Steel Company, Latrobe, Pennsylvania. The elemental iron and nickel powders were prepared by National Radiator Corporation, Johnstown, Pennsylvania, and the International Nickel Company, New York, New York, respectively. The various grades of electrolytic chromium were supplied by Electro Metallurgical Company, Niagara Falls, New York. The designated particle size of the various dispersants was -325 mesh; however, the actual particle size of the elemental powders was somewhat less. The results of chemical analyses on the prealloyed stainless steels are listed in Table III. The major impurities in the elemental powders were determined by chemical analysis and appear in Table IV. Particular emphasis was given to the silicon content of the material; for this reason a summary of the silicon content for each dispersant is presented in Table V.

III. PREPARATION OF POWDER METALLURGY TEST COMPACTS

The specimens used in evaluating the compatibility of Eu_2O_3 in silicon-bearing stainless steels were prepared by conventional powder metallurgical techniques. The compacts contained approximately 30 weight per cent Eu_2O_3—balance dispersant and weighed about 1.530 grams.

TABLE III

CHEMICAL COMPOSITION OF THE PREALLOYED STAINLESS STEEL DISPERSANTS EMPLOYED IN THE COMPATIBILITY TESTS

Type of Stainless Steel	Weight Per Cent						
	Cr	Ni	Mn	C	Si	P	S
304B	18.04	10.25	0.87	0.06	2.34	0.013	0.010
347B*	18.62	10.73	0.81	0.07	2.08	0.010	0.008
304L	17.22	11.12	0.40	0.04	0.11	0.008	0.022
304LB	18.28	8.64	0.93	0.02	1.95	0.013	0.013
304	18.26	9.11	1.12	0.05	0.22	0.015	0.006

*Niobium content of steel 0.94 per cent.

TABLE IV

CHEMICAL COMPOSITION OF THE VARIOUS ELEMENTAL DISPERSANTS

Element	Weight Per Cent						
	Fe	C	O_2	Mn	Si*	P	S
Plast-Iron	99.66	0.03	0.28	0.002	< 10 ppm	0.005	0.007
Carbonyl-Nickel	0.003	0.1		0.002	< 10 ppm		< 75 ppm
Type I-Chromium	0.022	0.02	0.71		28 ppm		0.024
Type II-Chromium	0.37	0.07	0.24		0.12		0.03
Type III-Chromium	0.04	0.03	0.56		58 ppm		0.037

*Accuracy of silicon analysis in the 30 ppm range ± 20 wt %.

TABLE V

SILICON CONTENT OF THE DISPERSANT MATERIALS

Type of Dispersant	Silicon Content
Stainless Steel-Type 304B	2.34 wt %
Stainless Steel-Type 347B	2.08 wt %
Stainless Steel-Type 304L	0.11 wt %
Stainless Steel-Type 304LB	1.95 wt %
Stainless Steel-Type 304	0.22 wt %
Plast-Iron	< 10 ppm
Carbonyl-Nickel	< 10 ppm
Type I-Chromium	28 ppm
Type II-Chromium	0.12 wt %
Type III-Chromium	58 ppm

The various types of Eu_2O_3 and dispersants were blended on an oblique-type blender for three hours to obtain a homogeneous mixture. No blending additives such as alcohol or carbon tetrachloride were employed in the process. The compacts were consolidated by cold pressing in double-acting powder metallurgy dies of one-fourth and five-sixteenths inch diameters. Two type pressing cycles were employed: (1) the single cold compaction of the blended powders at 33 tons per square inch pressure, and (2) the pre-cold compaction of the blended powders at 10 tons per square inch pressure followed by a compaction at 33 tons per square inch pressure after an initial sintering. A wide variety of compact dimensions was obtained depending mostly on the type of dispersant. Employing a single step cold press, the compact dimensions for the prealloyed stainless steel base dispersions were normally 0.252 inch diameter and 0.300 inch high.

IV. POWDER COMPACT HEAT TREATMENT AND VOLUME CHANGE MEASUREMENTS

The heat treatment of the various powder metallurgy compacts was conducted in a manner to establish the effect of heat-treating temperature, time, and atmosphere on the stability of Eu_2O_3 in silicon-bearing stainless steels. Compacts containing an identical type of oxide dispersed in different matrices of varying silicon content were also heat treated under identical conditions to establish the role of silicon content on the general stability of the Eu_2O_3. Along with establishing the effect of silicon, the conditioning treatment of the europium oxide was also investigated.

The general heat-treating parameters of the various tests covered times ranging from one and one-half to sixteen hours, temperatures from 900 to 1250°C, and furnace atmospheres of argon, helium, hydrogen, and vacuum. The heat treating was performed in a 3 inch diameter by 24 inch Globar-type furnace capable of extended use at 1250°C. The individual specimens were inserted into the hot zone of the Inconel muffle through the port door attached at the end of the cold zone. While specimens were either being inserted or removed from the furnace, a constant purge of helium was employed to prevent condensation of water vapor. The various gases employed as a furnace atmosphere were thoroughly dried and their dew point measured by a Beckman Hydrometer. The inlet dew point of the various gases was normally -62°C. The vacuum heat treatments were conducted in a similar type furnace where a quartz muffle attached to an evacuation system was employed.

Prior to heat treatment, the individual powder metallurgy prepared compacts were weighed on a Gram-o-matic balance and their dimensions obtained with a micrometer. Upon completing these initial measurements, which served as bases for observing the heat-treating changes, the compacts were placed in a molybdenum-lined ceramic boat. The molybdenum was employed to prevent contact of the Eu_2O_3-bearing compacts with the ceramic boats which were found to contain considerable amounts of silicon, mostly in compound form.

Upon completion of the heat treatment, the ceramic boat was removed from the hot zone and allowed to cool in the cold zone of the muffle under the same atmosphere. When the compact was sufficiently

cool to handle, the boat was removed from the muffle through the port door and visually examined for reaction products. The individual specimens were again weighed on the same balance and external dimensions remeasured. The weight change of the specimen was then obtained along with the volume change expressed in a percentage of the original volume. All pertinent observations and measured values were recorded.

V. REACTION PRODUCT IDENTIFICATION

A qualitative determination of the extent of reaction was obtained by the volume changes in the heat-treated specimens. A further determination of the compatibility of the Eu_2O_3 in the various dispersants was made by metallographic examinations. The individual heat-treated specimens were sectioned and a portion carefully mounted to prevent breakup and possible loss of the reaction products. The mounted specimens were then prepared for examination employing techniques developed by DuBose (11). In brief, the process consisted of a rough hand polish followed by vibratory polishing with Linde "A" type Al_2O_3 using a water-free silicone oil as a lubricant. Caution was exercised throughout the metallographic preparation to prevent possible contact of the specimens with water. Both bright-field illuminations and polarized light were employed in the subsequent metallographic examinations. In a few instances for further clarity of the oxide-dispersant boundary, Formvar-Au-Manganin replicas were prepared for electron microscopy.

In specimens which possessed considerable quantities of reaction products, attempts were made to remove the products by microchiseling.

This process did not yield single products, but merely aided in concentrating the products to facilitate x-ray examination. Attempts were also made to obtain x-ray diffraction patterns from the polished surfaces of the specimens as well as from powder samples obtained by crushing a portion of the heat-treated compact. In all cases, identification of the unknown diffraction lines was attempted by comparison to available standards. Since silicon was considered as the principle cause for the instability of Eu_2O_3 in stainless steel, x-ray standards of the various europium-silicon compounds were essential. Thus, a basic evaluation of the silicon-europium system was undertaken.

A series of europium-silicon alloys ranging in composition from 3–90 atomic per cent europium were prepared by arc melting. Since europium metal oxidizes rapidly when exposed to air, the material was prepared for melting in a helium atmosphere dry box. Transfer of the materials from the dry box to the arc furnace was accomplished in gas-tight bottles. To minimize air exposure while positioning the weighed charge on the copper melting hearth, the furnace interior was purged with helium upon completion of the charging, the furnace was sealed and evacuated to approximately one micron. This evacuation was repeated after the furnace had been purged with high-purity argon. Prior to arc melting the experimental alloys, a zirconium button was melted in order to reduce the moisture and oxygen content in the argon atmosphere. The individual charges were then arc melted twice in an effort to obtain homogeneous alloys. Samples of the cast alloys were then submitted for x-ray, chemical, and metallographic evaluations. A portion of several alloys was also heat treated at 750°C for 72 hours. To

prevent possible contamination of the alloys during heat treatment, the material was encased in tantalum foil, surrounded with molybdenum foil and inserted in an evacuated quartz capsule. A small piece of zirconium foil was also inserted between the specimen and molybdenum foil to serve as an oxygen "getter." After heat treating, the various alloys were removed from the quartz capsules and evaluated for structural and chemical changes. Similar type specimens were also encapsulated in nickel tubes and heat treated.

CHAPTER VI

RESULTS AND DISCUSSION

The effect of silicon on the stability of Eu_2O_3 in stainless steel was demonstrated by the heat treatment of powder metallurgy compacts of varying silicon content. Similar tests were also conducted to evaluate the effect of heat-treating time, temperature, and atmosphere, and the initial oxide conditioning treatment on the compatibility of the Eu_2O_3-bearing dispersions. The general effect of silicon on the stability of Eu_2O_3 in stainless steel and other dispersants can be seen in Table VI. The individual specimens contained type D-Eu_2O_3 (conditioned by firing at 1700°C in hydrogen for three hours) dispersed in matrices of varying silicon content. The heat treatment was conducted at 1230°C for one and one-half hours in a hydrogen atmosphere of -62°C dew point. In general, the stability of the Eu_2O_3 appeared to decrease as the silicon content in the dispersant increased. The instability was manifested by a volume increase in the compact and the appearance of a thin film which coated the specimen and various surfaces of the molybdenum sintering boats. The film had a distinct yellow-green appearance in all cases. The complete absence of this film was noted on the boats where direct contact of the sample had occurred during heating. In these areas no detectable reaction was observed between the molybdenum and compact constituents.

Although the stability of the oxide appears to increase, in general, with decreasing silicon content, certain anomalies are present in the data. Compacts containing type 304L stainless steel were found

TABLE VI

EFFECT OF SILICON ON THE STABILITY OF Eu_2O_3 IN VARIOUS MATRIX MATERIALS

Matrix Material	Silicon Content (wt%)	Weight Change (g)	Volume Change (%)	Remarks
Stainless Steel-Type 304B	2.34	-0.0038	+ 6.30	Specimen covered with yellow-green film
	2.34	-0.0041	+ 6.89	Specimen covered with yellow-green film
	2.34	-0.0033	+ 6.58	Specimen covered with yellow-green film
Stainless Steel-Type 347B	2.08	-0.0050	+ 5.35	Specimen covered with yellow-green film
	2.08	-0.0078	+ 3.41	Specimen covered with yellow-green film
	2.08	-0.0073	+ 3.53	Specimen covered with yellow-green film
	2.08	-0.0071	+ 3.53	Specimen covered with yellow-green film
Stainless Steel-Type 304L	0.11	-0.0051	- 4.22	Specimen lightly covered with yellow-green film
	0.11	-0.0064	- 3.89	Specimen lightly covered with yellow-green film
	0.11	-0.0067	- 3.12	Specimen lightly covered with yellow-green film
	0.11	-0.0066	- 3.38	Specimen lightly covered with yellow-green film
Plast-Iron	< 10 ppm	-0.0085	- 2.05	Specimen appeared metallic
	< 10 ppm	-0.0090	- 2.13	Specimen appeared metallic
Carbonyl-Nickel	< 10 ppm	-0.0050	-14.15	Specimen appeared metallic
	< 10 ppm	-0.0061	-13.89	Specimen appeared metallic
	< 10 ppm	-0.0058	-14.53	Specimen appeared metallic
Type I-Chromium	28 ppm	-0.0035	- 2.69	Specimen appeared metallic
	28 ppm	-0.0039	- 2.34	Specimen appeared metallic

TABLE VI (continued)

Matrix Material	Silicon Content (wt%)	Weight Change (g)	Volume Change (%)	Remarks
Type II-Chromium	0.12	-0.0040	+ 1.72	Specimen covered with yellow-green film
	0.12	-0.0035	+ 2.02	Specimen covered with yellow-green film
Type III-Chromium	58 ppm	-0.0036	- 4.97	Specimen very slightly covered with yellow-green film
	58 ppm	-0.0030	- 5.36	Specimen very slightly covered with yellow-green film
	58 ppm	-0.0040	- 2.08	Specimen very slightly covered with yellow-green film
Elemental Fe-Ni-Type I-Cr		-0.0059	0.00	Specimen appeared metallic
		-0.0059	+ 0.07	Specimen appeared metallic
Elemental Fe-Ni-Type II-Cr		-0.0061	+ 2.27	Specimen covered with yellow-green film
		-0.0057	+ 2.13	Specimen covered with yellow-green film
Elemental Fe-Ni-Type III-Cr		-0.0058	- 0.34	Specimen appeared metallic
		-0.0053	+ 0.11	Specimen appeared metallic
Stainless Steel-Type 304	0.22		+ 2.60	Specimen slightly covered with yellow-green film
	0.22		+ 2.80	Specimen slightly covered with yellow-green film
	0.22		+ 2.93	Specimen slightly covered with yellow-green film
	0.22		+ 2.76	Specimen slightly covered with yellow-green film
Eu_2O_3-Type D (conditioned at 1700°C for three hours under hydrogen)				

relatively stable as manifested by the consistent volume decreases upon heat treating, while compacts containing type II-chromium were found to react. Both materials possessed the same relative amount of silicon. The reaction noted in the type II-chromium compacts, however, was less than that observed in the prealloyed, higher, silicon content stainless steels. Even though volume decreases were noted in the type 304L stainless steel compacts, the specimens were slightly coated with a yellow-green film after heat treating. A comparison of the results from the type I-chromium compacts with those of the type III-chromium also showed a similar anomaly for a greater degree of shrinkage was noted in the higher silicon-bearing material. The data obtained from heat treating the elemental compacts containing the various types of chromium appeared in order, although very slight volume increases were noted in the elemental compacts containing the type I- and type III-chromium. These volume increases are probably the result of entrapped gas expansion during heat treatment and not the result of a reaction. Such an effect has been observed in elemental-type steels and certain other base materials when too large an initial cold-pressing pressure has been employed. Decreasing the initial pressing pressure to 10 tons per square inch in place of the 33 tons per square inch resulted in a volume snrinkage for both type chromium-bearing compacts.

Along with evaluation of the stability of the Eu_2O_3 in materials of varying silicon content by volume changes, each heat-treated compact was examined metallographically. The examinations were conducted to establish the microstructural changes and their correlation with the volume changes. The reaction noted in the Eu_2O_3-type 304B stainless

steel compact after being heat treated for one and one-half hours at 1230°C can be seen in Figure 2. Each steel particle appears to be surrounded by a reaction product; the formation of a reaction product in the oxide particles is also evident. This product which appears as the darker areas in the generally grey regions of the photomicrograph is extremely difficult to retain during metallographic preparation. In fact, the initial preparations failed to show this phenomenon. The difficulty in retaining this product was subsequently attributed to its high degree of water solubility which was demonstrated by examining a particular region of the compact before and after a drop of demineralized degassed water was applied to the surface. Such an evaluation can be made by closely comparing the microstructure of Figure 3 to that shown in Figure 2. The dark grey areas, which appear dispersed in the light grey regions of Figure 2, have completely disappeared in Figure 3. The reaction product, however, observed around the individual steel particles is still present, indicating that the two phases or reaction products are basically different. The soluble product had a characteristic ruby-red appearance under bright-field illumination. A considerably larger formation of this red product as illustrated in Figure 4 was noted in the type 347B stainless steel compacts. Nearly all of the initial Eu_2O_3 particles were converted to this soluble product. As previously noted in the type 304B stainless steel compacts, a second reaction product can be observed around the individual stainless steel particles.

In an attempt to establish the identity of this soluble product, a reacted compact was exposed to a drop of water and the water subsequently spectrographically analyzed for base elements. As indicated in

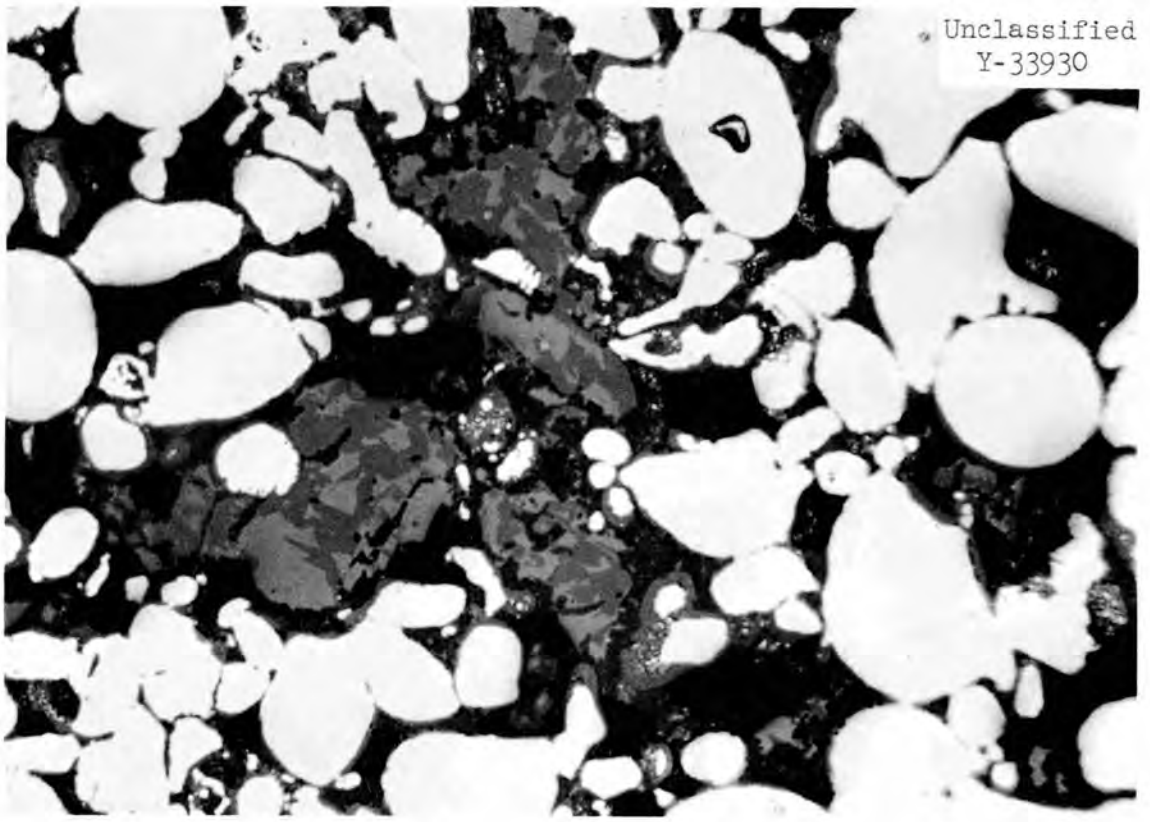

Figure 2. Microstructure of a 30 weight per cent type D-Eu_2O_3 dispersion in type 304B stainless steel heat treated at 1230°C for one and one-half hours under hydrogen. As polished. 500X.

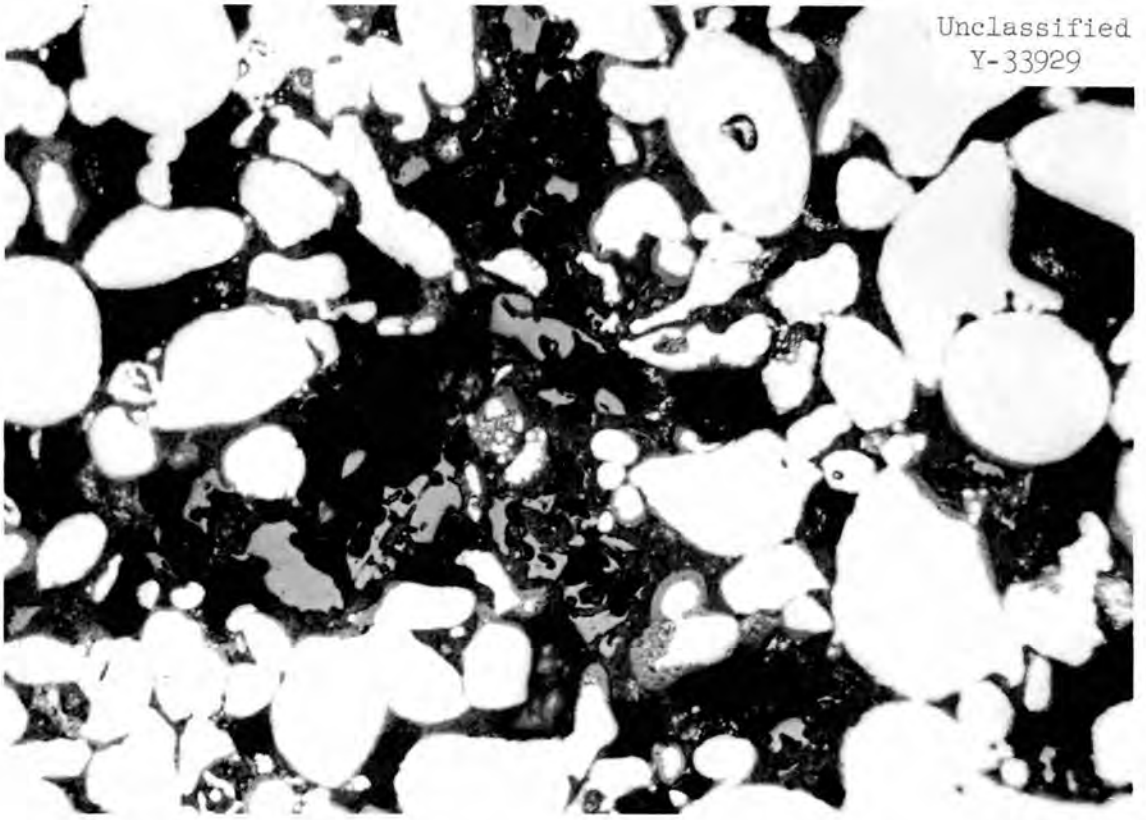

Figure 3. Same as Figure 2 except for being exposed to demineralized-distilled water. As polished. 500X.

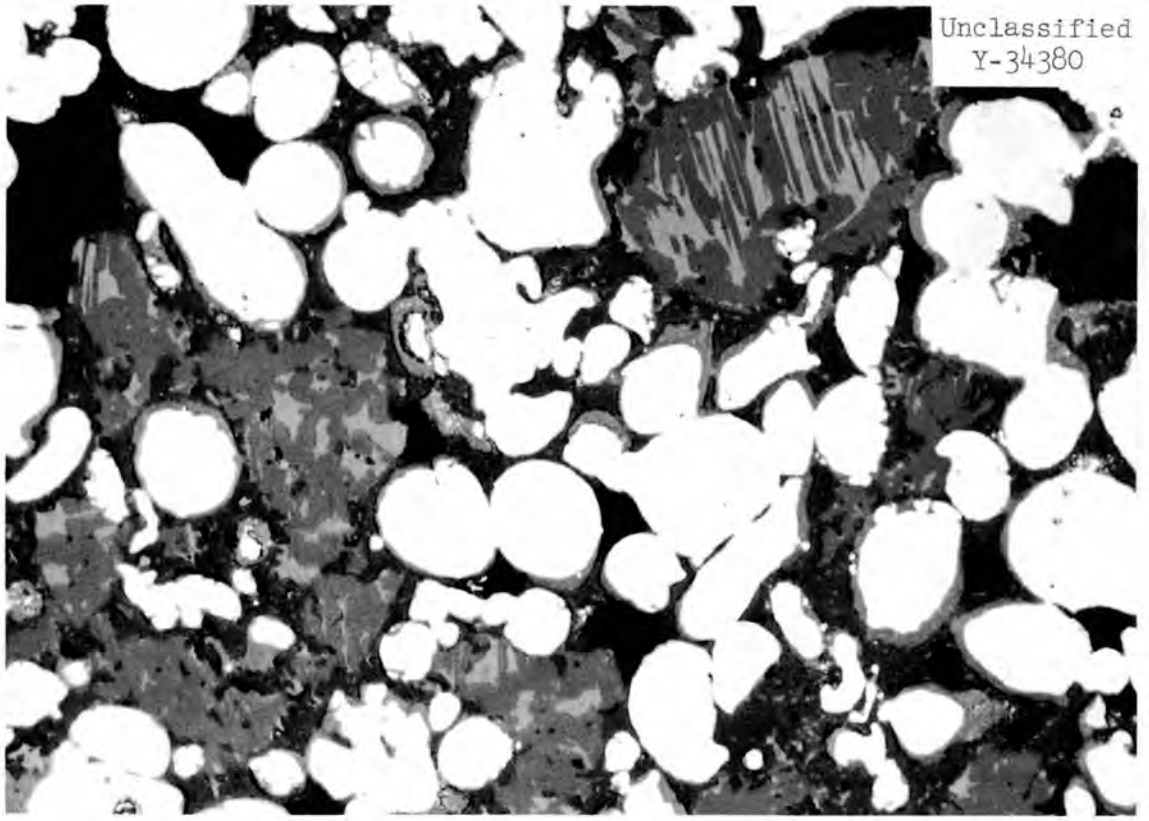

Figure 4. Microstructure of a 30 weight per cent type D-Eu_2O_3 dispersion in type 347B stainless steel heat treated at 1230°C for one and one-half hours under hydrogen. As polished. 500X.

Table VII, the solution was very strong in europium, a faint trace of silicon was also observed along with strong calcium and sodium contents. It was therefore concluded that the soluble phase in the relatively insoluble high-fired Eu_2O_3 was not a tramp phase but that it was europium bearing. Further attempts to identify this phase by x-ray diffraction did not prove successful, largely because of the lack of necessary standards.

Unlike the high silicon-type stainless steels, good stability of Eu_2O_3 was observed in most of the low silicon content matrix materials. Figure 5 illustrates a typical microstructure of the nickel-base compacts. No reaction products were noted at the oxide-nickel interfaces nor was there any formation of a second phase in the conditioned Eu_2O_3 particles. These particular compacts possessed the largest densification of all the material combinations tested.

The microstructure of a Eu_2O_3-type I-chromium compact is illustrated in Figure 6. Unlike the nickel-base dispersions, the formation of a surface layer can be seen on the periphery of the Eu_2O_3 particles. This layer appeared lighter in color than the grey oxide and seemed quite stable in regions of contact with the white-appearing chromium particles. The soluble phase observed in the oxide of the high silicon-bearing stainless steel compacts was not observed in the type I-chromium-base dispersions. The thin film formation around the Eu_2O_3 is not felt to be associated with silicon but is rather the possible interaction of a chromium oxide and Eu_2O_3 to form $EuCrO_3$. Such type reactions have been observed as previously referenced. Figure 7 illustrates that an identical interaction occurred between the Eu_2O_3

TABLE VII

SPECTROGRAPHIC ANALYSIS OF H_2O REMOVED FROM SURFACE OF A REACTED Eu_2O_3-TYPE 304B STAINLESS STEEL COMPACT

Element	Concentration
Al	Faint trace
B	Very weak
Ca	Strong
Eu	Very strong
Fe	Trace
Mg	Weak
Mn	Faint trace
Na	Strong
Si	Very weak
Sn	
Ti	
V	

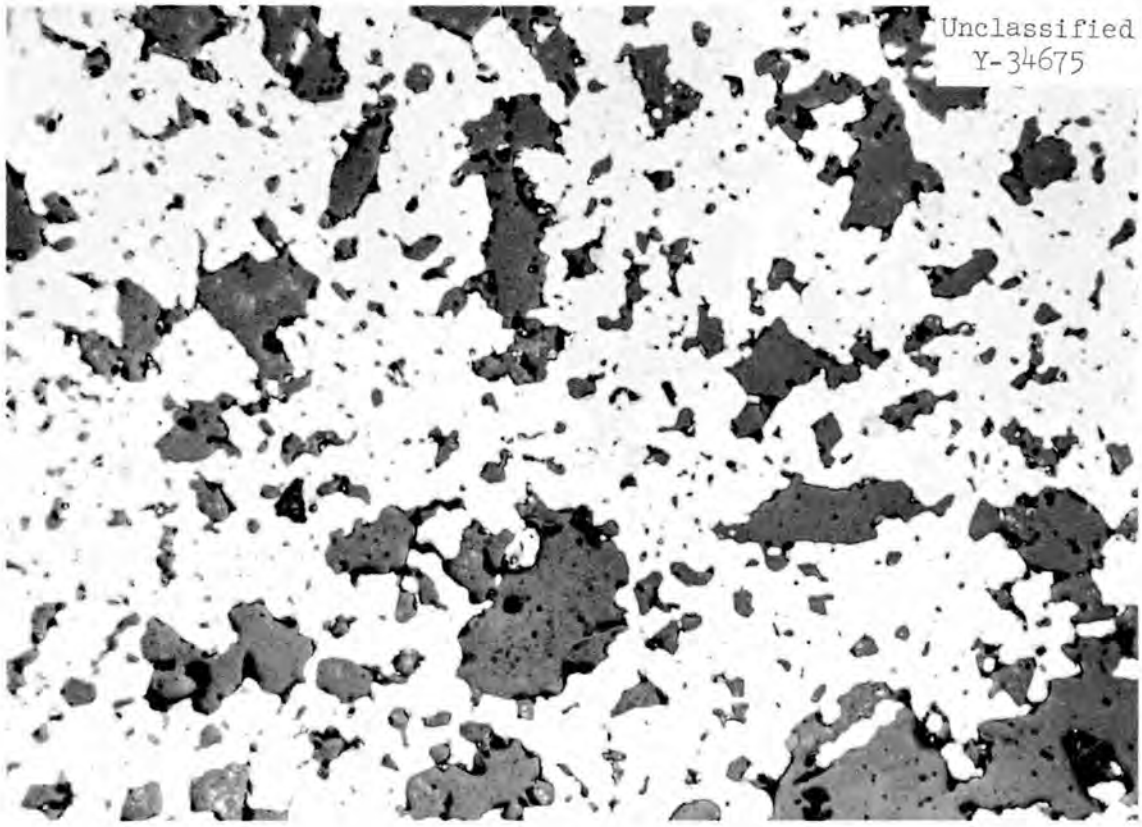

Figure 5. Microstructure of a 30 weight per cent type D-Eu_2O_3-nickel compact heat treated at 1230°C for one and one-half hours under hydrogen. As polished. 500X.

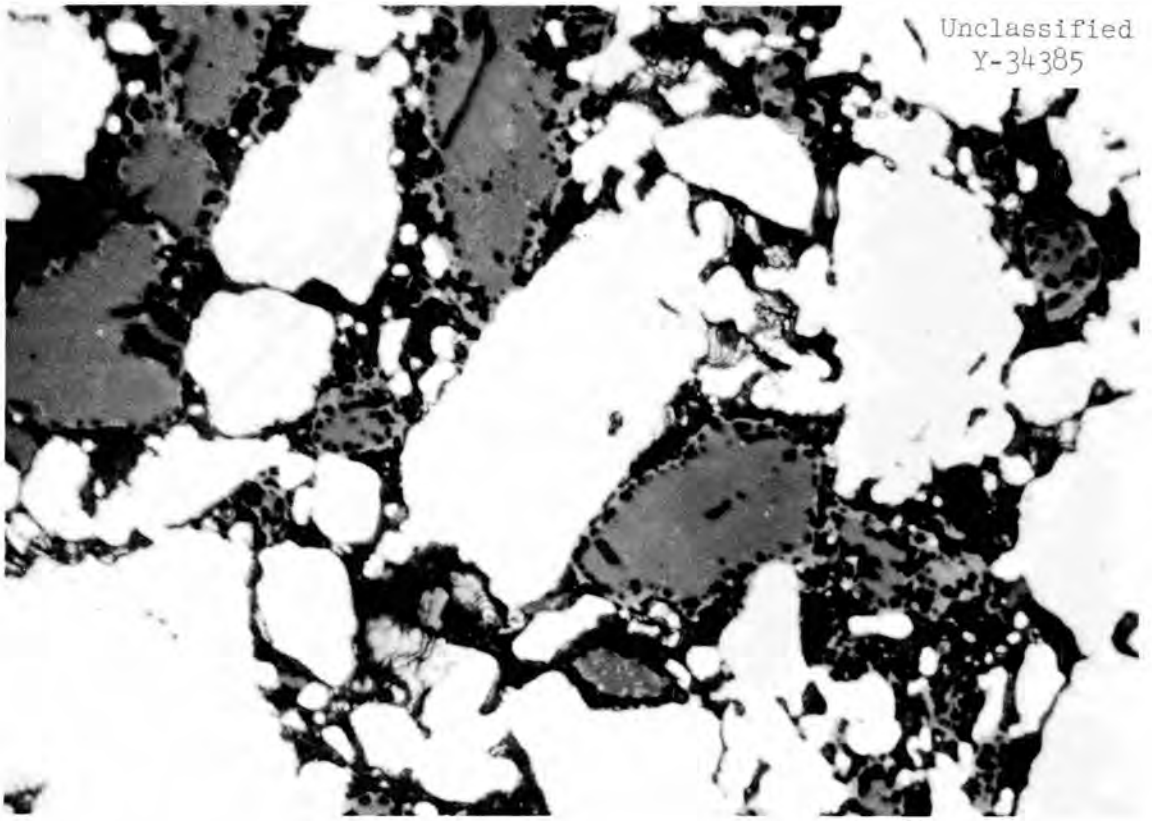

Figure 6. Microstructure of a 30 weight per cent type D-Eu_2O_3 dispersion in type I-chromium heat treated at 1230°C for one and one-half hours under hydrogen. As polished. 1000X.

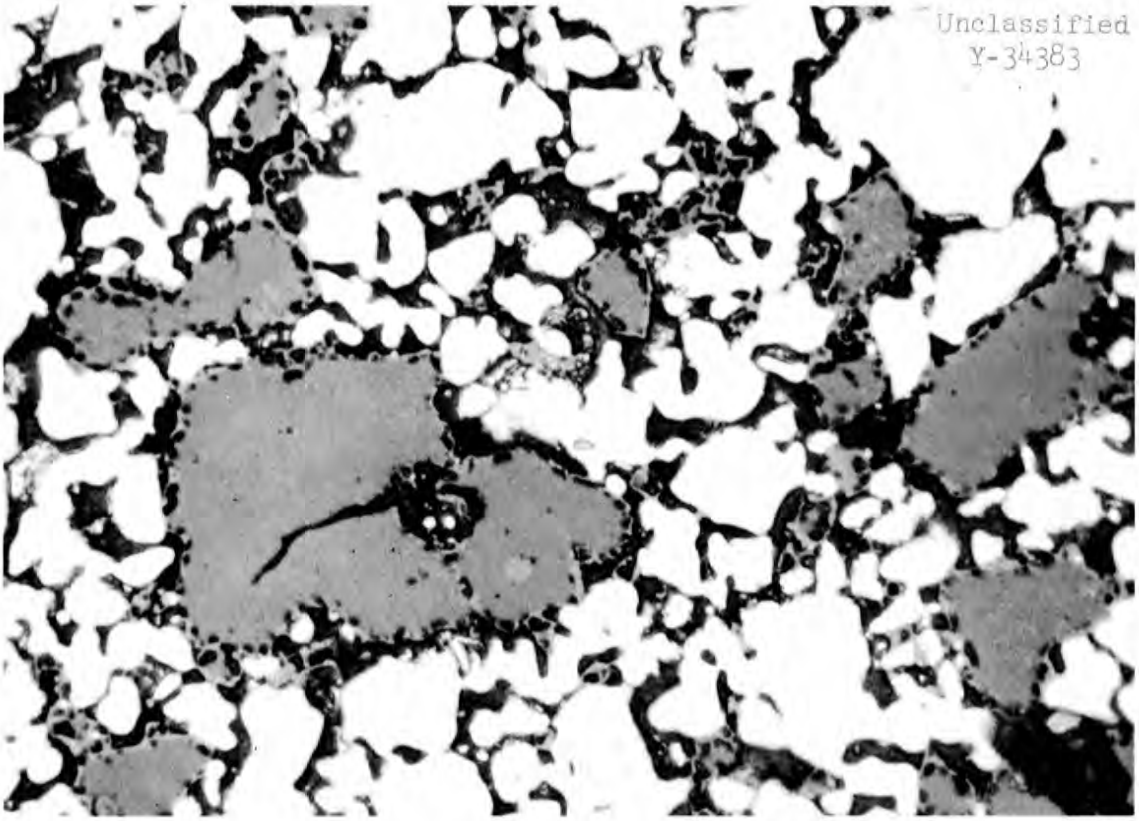

Figure 7. Microstructure of a 30 weight per cent type D-Eu_2O_3 dispersion in type III-chromium heat treated at 1230°C for one and one-half hours under hydrogen. As polished. 1000X.

and the type III-chromium when heat treated at 1175°C for one and one-half hours under hydrogen. However, the type I-chromium-bearing compacts appears to have a slightly larger reaction band. It was interesting to note that a higher oxygen content was present in the type I-chromium. This interaction between the chromium and Eu_2O_3 is not very evident in the type II-chromium-bearing compacts, as illustrated in Figure 8. The peripheral band is not observed and instead a band of particles appears only at chromium oxide interfaces. No soluble phase was noted in the Eu_2O_3 particles even though a compact volume increase and film formations were noted on heating. Identical type effects were also noted in the elemental stainless steel compacts containing the various types of chromium; however, in these cases a slight film was noted on portions of the individual particles in the type II-chromium-bearing dispersions. This film was similar to the films noted earlier in the stainless steel, high silicon-bearing dispersions. These films were not observed in either the type I- or type III-chromium-bearing elemental steel dispersions when heat treated at 1230°C for one and one-half hours under a hydrogen atmosphere.

To clarify the reactions noted between type D-Eu_2O_3 and various matrix materials, similar type compacts containing identical matrix materials and the various types of Eu_2O_3 were heat treated. The individual compacts which contained approximately 30 weight per cent oxide were prepared by cold pressing at 33 tons per square inch pressure unless otherwise stated. The pressed compacts were heat treated at 1230°C for one and one-half hours under both a hydrogen and helium atmosphere. These were employed to establish whether the heat-treating

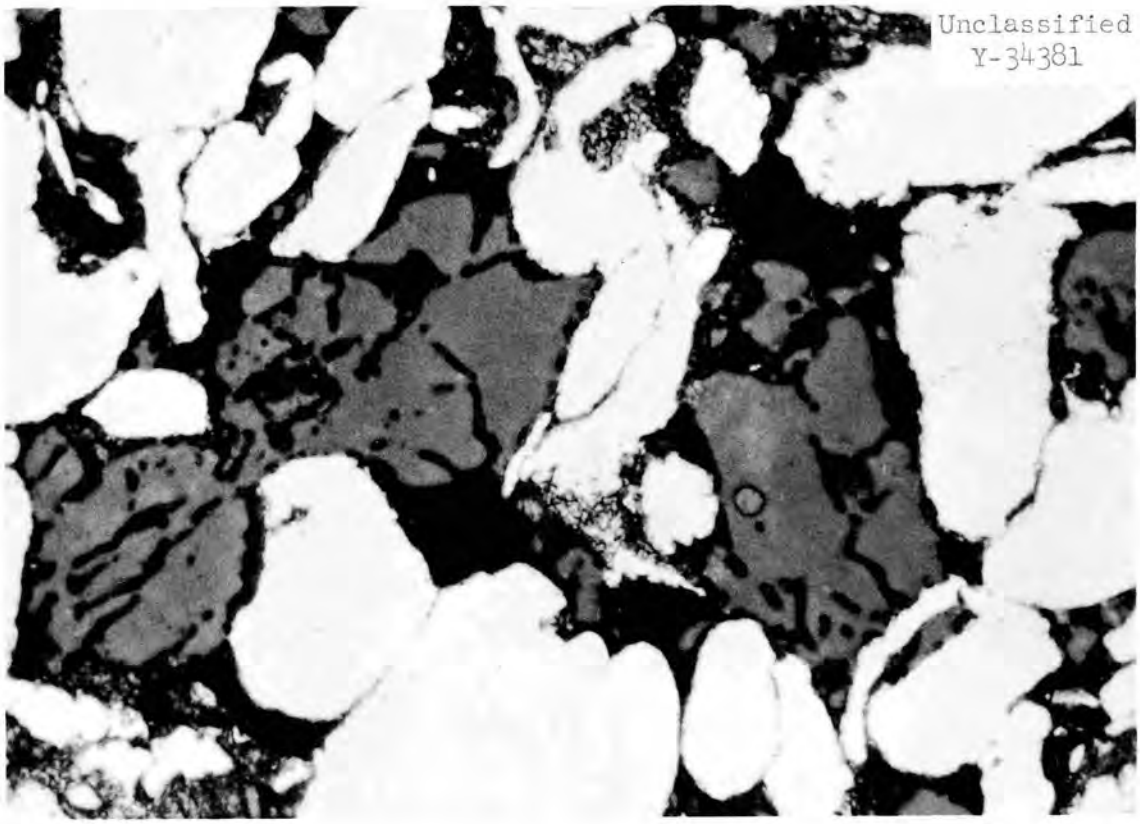

Figure 8. Microstructure of a 30 weight per cent type D-Eu_2O_3 dispersion in type II-chromium heat treated at 1230°C for one and one-half hours under hydrogen. As polished. 1000X.

atmosphere had an effect on the stability of the Eu_2O_3 in silicon-bearing matrix materials. The results obtained from the heat treatment of the various type Eu_2O_3-bearing dispersions in hydrogen and in helium are shown in Tables VIII and IX, respectively. In the tests performed, no noticeable effect of oxide conditioning was observed on the stability of the Eu_2O_3 in the various silicon-bearing dispersants. The magnitude of the volume change measured on the compacts heat treated in hydrogen compared favorably with the data presented in Table VI, page 28, independent of the conditioning treatment of the Eu_2O_3. The specimen containing the as-received Eu_2O_3 dispersed in type 304B stainless steel was cold compacted at ten tons per square inch pressure; therefore, the magnitude of the volume change was not comparable to the remaining data. A positive reaction, however, was noted in this specimen. It is important to realize that the volume changes reported provide only supplementary qualitative information concerning the reaction since such effects as matrix oxide reduction and compact sintering are encountered during the heat treatments. Both effects have a tendency to reduce the over-all compact volume.

Although similar reaction behavior is indicated in Table IX, a considerably larger spread in the data existed than for the heat treatments in hydrogen atmospheres. Heat treating in a helium atmosphere appeared to result in smaller volume increases as manifested by a comparison of the data in Tables VIII and IX. The various type Eu_2O_3-304B compacts when heat treated in hydrogen had a volume increase in the range 6.30–7.98 per cent, whereas, the helium-treated specimens had a volume increase ranging from only 0.92–2.45 per cent. Similar

TABLE VIII

EFFECT OF OXIDE CONDITIONING ON STABILITY OF Eu_2O_3 IN VARIOUS DISPERSANTS HEAT TREATED AT 1230°C UNDER HYDROGEN

Type Oxide	Dispersant	Weight Change (g)	Volume Change (%)	Remarks
A*	Stainless Steel-Type 304B	-0.0510	+ 2.08	Specimen covered with yellow-green film
B	Stainless Steel-Type 304B	-0.0039	+ 7.98	Specimen covered with yellow-green film
C	Stainless Steel-Type 304B	-0.0039	+ 7.96	Specimen covered with yellow-green film
D	Stainless Steel-Type 304B	-0.0038	+ 6.30	Specimen covered with yellow-green film
E	Stainless Steel-Type 304B	-0.0018	+ 7.05	Specimen covered with yellow-green film
B	Stainless Steel-Type 347B	-0.0036	+ 5.81	Specimen covered with yellow-green film
C	Stainless Steel-Type 347B	-0.0036	+ 5.55	Specimen covered with yellow-green film
D	Stainless Steel-Type 347B	-0.0050	+ 5.35	Specimen covered with yellow-green film
E	Stainless Steel-Type 347B	-0.0028	+ 6.96	Specimen covered with yellow-green film
B	Nickel	-0.0042	-14.26	Specimen appeared metallic
C	Nickel	-0.0049	-14.26	Specimen appeared metallic
D	Nickel	-0.0050	-14.15	Specimen appeared metallic
E	Nickel	-0.0050	-14.91	Specimen appeared metallic
B	Stainless Steel-Type 304L	-0.0034	- 1.54	Specimen slightly tarnished
C	Stainless Steel-Type 304L	-0.0040	- 1.53	Specimen slightly tarnished

TABLE VIII (continued)

Type Oxide	Dispersant	Weight Change (g)	Volume Change (%)	Remarks
D	Stainless Steel-Type 304L	-0.0051	- 4.22	Specimen slightly tarnished
E	Stainless Steel-Type 304L	-0.0038	- 1.99	Specimen slightly tarnished
B	Type I-Chromium	-0.0034	- 2.39	Specimen appeared metallic
C	Type I-Chromium	-0.0037	- 2.68	Specimen appeared metallic
D	Type I-Chromium	-0.0035	- 2.69	Specimen appeared metallic
E	Type I-Chromium	-0.0025	- 2.39	Specimen appeared metallic
B	Type II-Chromium	-0.0026	+ 2.43	Specimen covered with yellow-green film
C	Type II-Chromium	-0.0027	+ 2.06	Specimen covered with yellow-green film

*Specimen initially cold pressed at 10 tsi pressure.

TABLE IX

EFFECT OF OXIDE CONDITIONING ON STABILITY OF Eu_2O_3 IN VARIOUS DISPERSANTS HEAT TREATED AT 1230°C UNDER HELIUM

Type Oxide	Dispersant	Weight Change (g)	Volume Change (%)	Remarks
A*	Stainless Steel-Type 304B	-0.0430	+ 0.53	Specimen covered with yellow-green film
B	Stainless Steel-Type 304B	-0.0022	+ 0.92	Specimen covered with yellow-green film
C	Stainless Steel-Type 304B	-0.0029	+ 1.53	Specimen covered with yellow-green film
D	Stainless Steel-Type 304B	-0.0046	+ 2.45	Specimen covered with yellow-green film
E	Stainless Steel-Type 304B	-0.0022	+ 1.78	Specimen covered with yellow-green film
B	Stainless Steel-Type 347B	-0.0029	+ 3.77	Specimen covered with yellow-green film
C	Stainless Steel-Type 347B	-0.0036	+ 2.39	Specimen covered with yellow-green film
D	Stainless Steel-Type 347B	-0.0053	+ 3.40	Specimen covered with yellow-green film
E	Stainless Steel-Type 347B	-0.0030	+ 1.60	Specimen covered with yellow-green film
D	Nickel	-0.0068	-17.02	Specimen appeared metallic
B	Stainless Steel-Type 304L	-0.0023	- 1.62	Specimen slightly covered with film
C	Stainless Steel-Type 304L	-0.0019	- 1.77	Specimen slightly covered with film
D	Stainless Steel-Type 304L	-0.0035	- 1.50	Specimen slightly covered with film
E	Stainless Steel-Type 304L	-0.0019	- 1.15	Specimen slightly covered with film

TABLE IX (continued)

Type Oxide	Dispersant	Weight Change (g)	Volume Change (%)	Remarks
B	Type II-Chromium	-0.0032	+ 0.83	Specimen covered with yellow-green film
C	Type II-Chromium	-0.0031	+ 0.49	Specimen covered with yellow-green film
D	Type I-Chromium	-0.0045	- 3.49	Specimen appeared metallic

*Specimen initially cold pressed at 10 tsi pressure.

differences between the volume changes in compacts heat treated in hydrogen and helium were seen in all of the tested matrix materials except in the type 304L stainless steel-base dispersions, where nearly identical volume changes were noted in both atmospheres.

As in hydrogen-treated compacts, the reaction in helium between the Eu_2O_3 and silicon-bearing matrix materials was manifested by the appearance of a yellow-green film which likewise coated various uncovered regions of the heat-treating boats. An x-ray diffraction pattern of this film was found identical with the patterns obtained from films formed under hydrogen.

The metallographic examination of the tested specimens also indicated that the appearance of the reaction between the Eu_2O_3 and the high silicon-bearing stainless steels was independent of initial oxide conditioning and heat-treating atmosphere. Figures 9 and 10 represent the microstructure of type D-Eu_2O_3 dispersed in types 304B and 347B stainless steels, respectively, after heat treatment at 1230°C for one and one-half hours under helium. A comparison of these figures with Figures 2, page 32, and 4, page 34, indicates similar reacted microstructures, although it can be seen that the degree of second phase formation in the Eu_2O_3 particles is considerably less in the helium-treated compacts. Correspondingly, smaller volume changes were noted in these materials when heat treated under helium. Figures 11 and 12 illustrate the microstructures of helium heat-treated types 304B and 347B stainless steel-base dispersions containing type B-Eu_2O_3. A comparison of these structures with those shown in Figures 9 and 10 failed to indicate any gross differences as a result of the different oxide conditioning treatments.

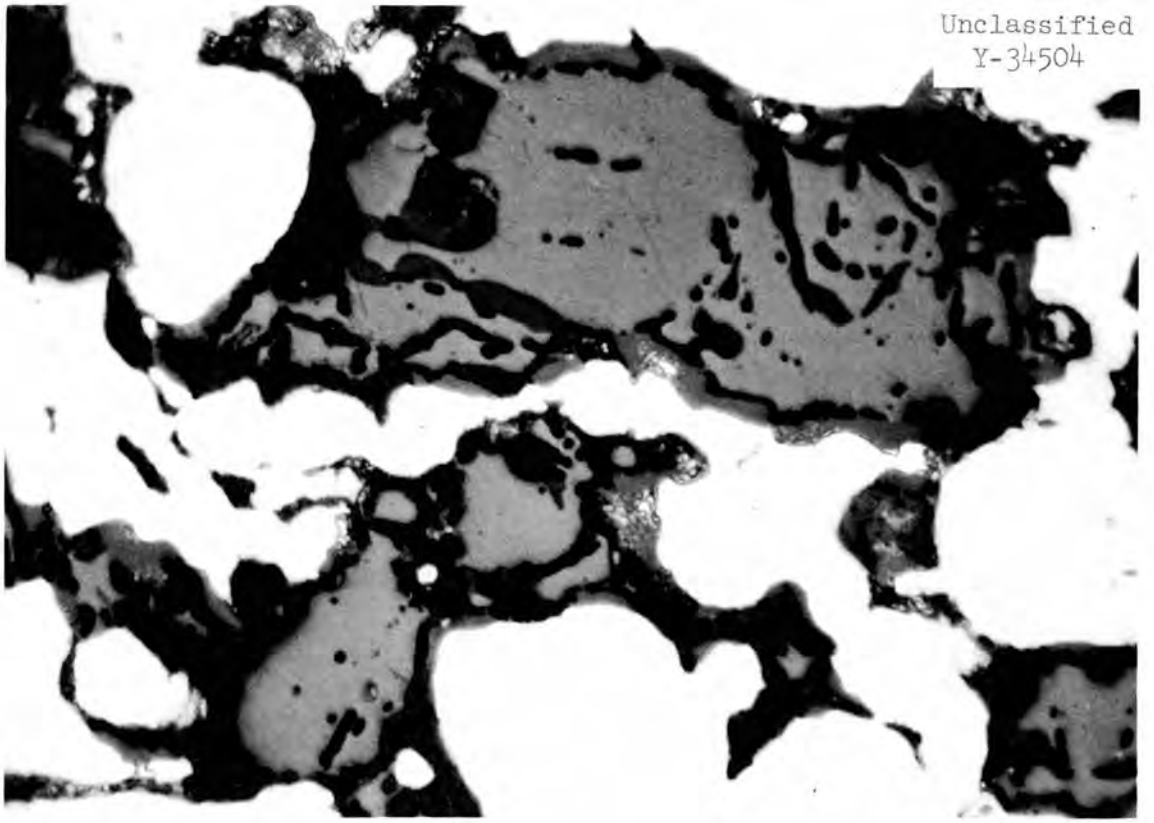

Figure 9. Microstructure of a 30 weight per cent type D-Eu_2O_3-type 304B stainless steel compact heat treated at 1230°C for one and one-half hours under helium. As polished. 1000X.

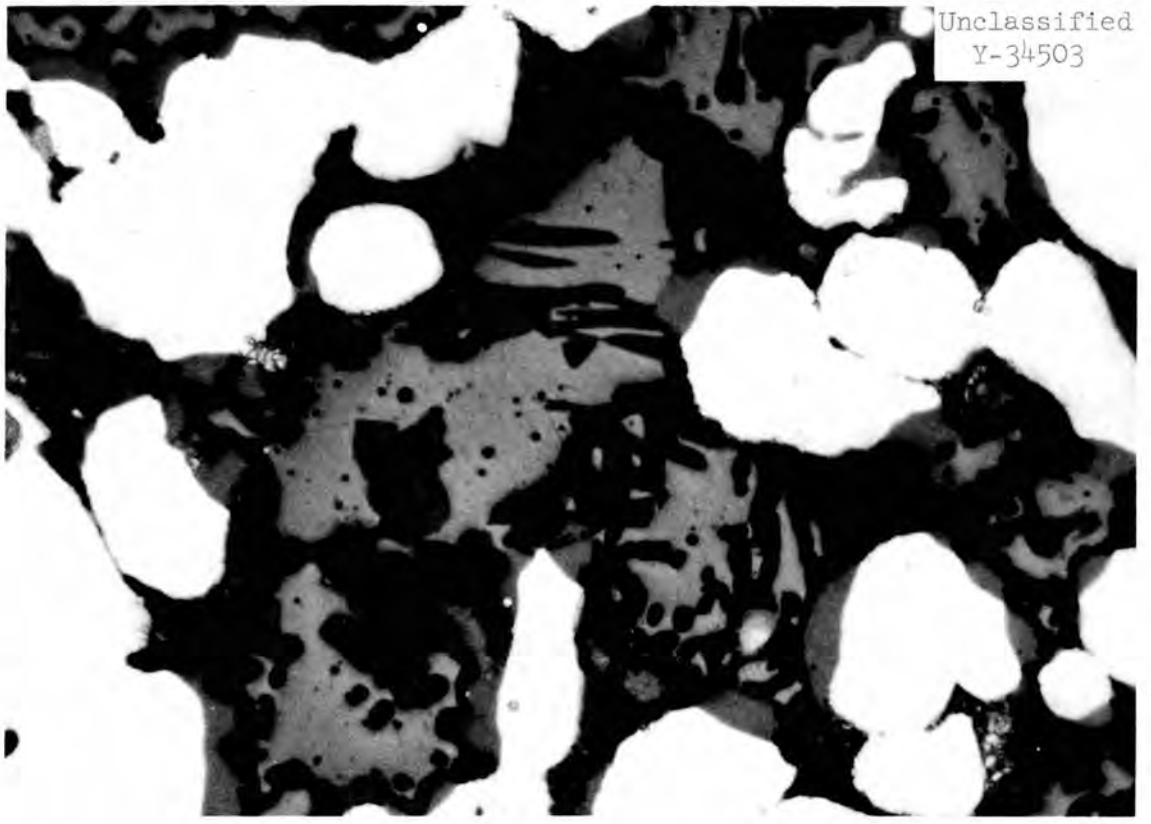

Figure 10. Microstructure of a 30 weight per cent type D-Eu_2O_3 dispersed in type 347B stainless steel and heat treated at 1230°C for one and one-half hours under helium. As polished. 1000X.

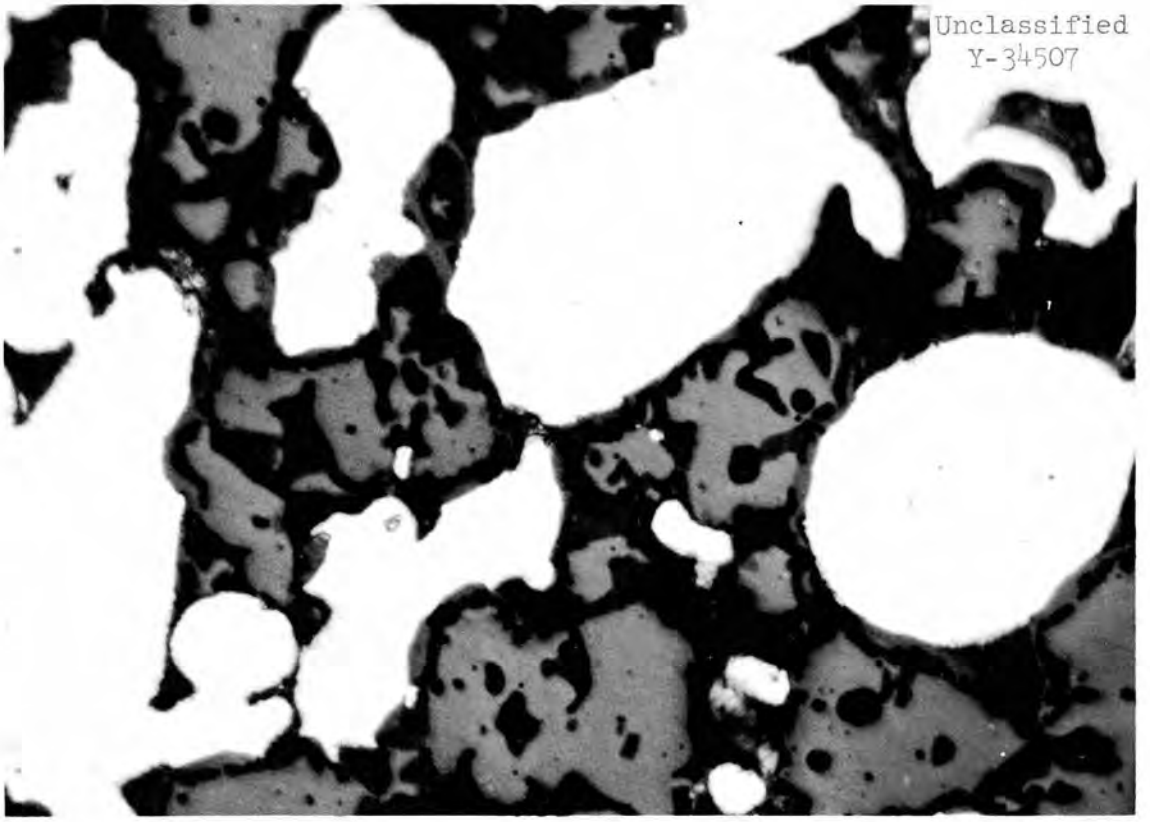

Figure 11. Microstructure of a 30 weight per cent type B-Eu_2O_3-304B stainless steel dispersion heat treated at 1230°C for one and one-half hours under helium. As polished. 1000X.

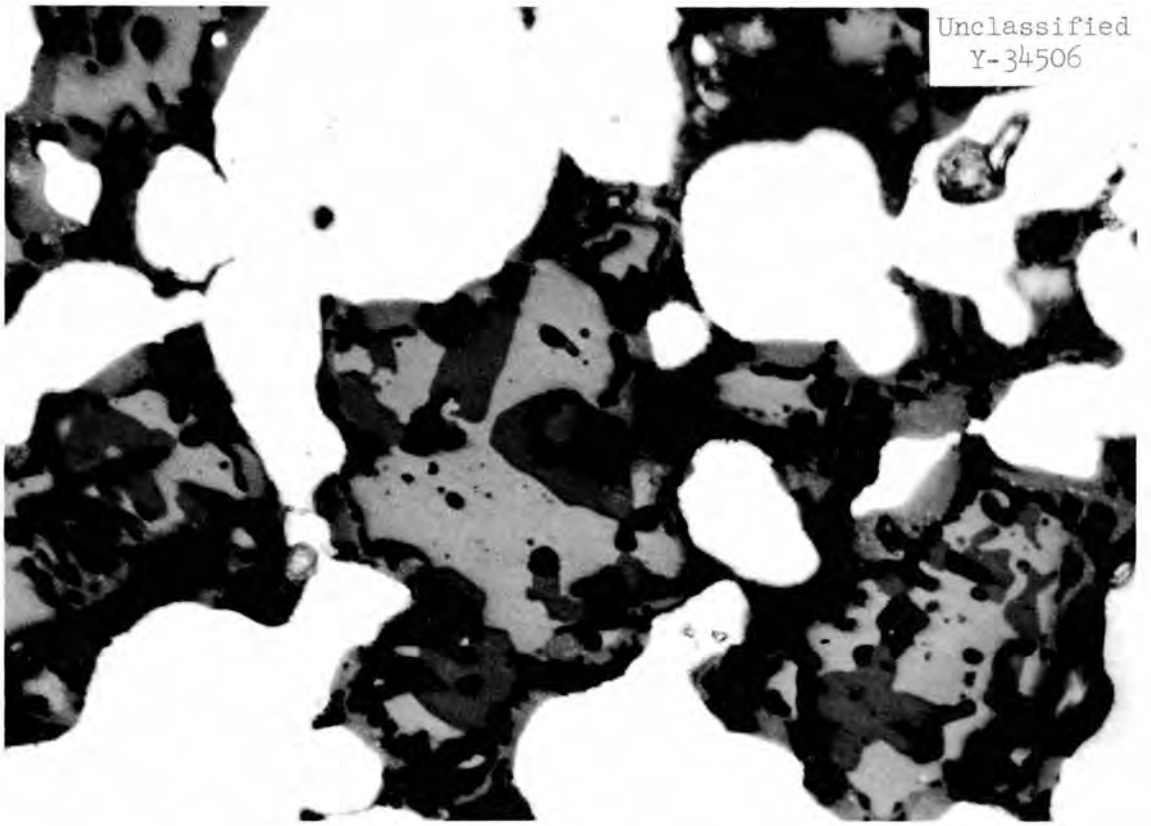

Figure 12. Microstructure of 30 weight per cent type B-Eu_2O_3 dispersed in type 347 stainless steel and heat treated at 1230°C for one and one-half hours under helium. As polished. 1000X.

Similar observations were also noted in the compacts containing the essentially, silicon-free dispersants. A general comparison of the microstructures represented in Figures 13, 14, and 15 for the nickel-base dispersions containing type E, type B, and type C-Eu_2O_3, respectively, failed to indicate any gross differences. Heat treating the nickel-base dispersions under helium, as indicated in Figure 16, also produced no observable changes in microstructure.

Microstructures similar to the higher silicon-bearing prealloyed stainless steels were observed in the type 304L stainless steel-base dispersions when heat treated under helium or hydrogen. The microstructures of compacts containing type D-Eu_2O_3 dispersed in type 304L stainless steel and heat treated at 1230°C for one and one-half hours under helium and hydrogen are shown in Figures 17 and 18, respectively. Examination of the microstructures showed that a small amount of deposit, common as a reaction product in the higher silicon-bearing steel dispersions, was present in localized regions on the periphery of the type 304L steel. However, no second phase formation was noted in the Eu_2O_3 particles. The presence of the peripheral deposit indicated that a slight reaction could have occurred during heat treatment and thus accounted for the presence of the yellow-green film even though a volume decrease was noted on heat treating. An interaction, similar to that observed in the chromium-base dispersions, also was observed between the Eu_2O_3 particles and the type 304L stainless steel. Identical type observations were likewise noted in compacts containing types B, C, and E-Eu_2O_3 dispersed in type 304L stainless steel when heat treated for one and one-half hours at 1230°C under either a helium or hydrogen atmosphere.

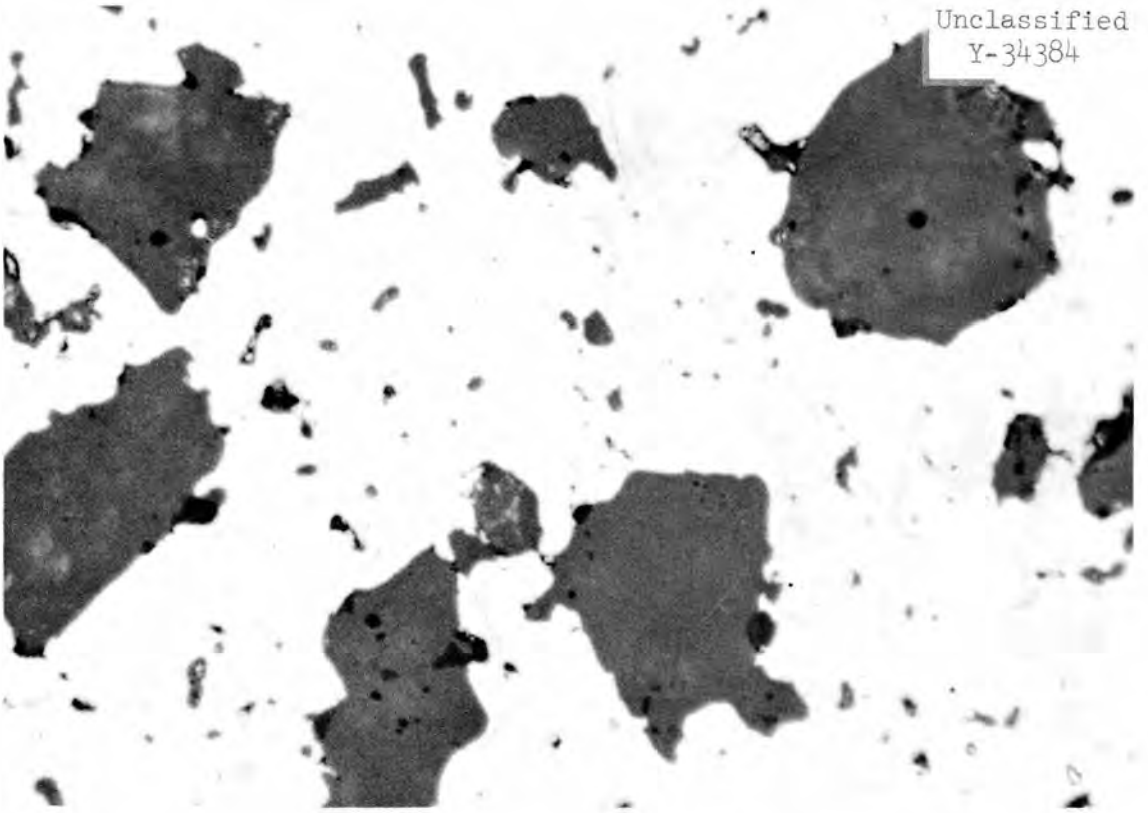

Figure 13. Microstructure of 30 weight per cent type E-Eu_2O_3 dispersed in nickel and heat treated at 1230°C for one and one-half hours under hydrogen. As polished. 1000X.

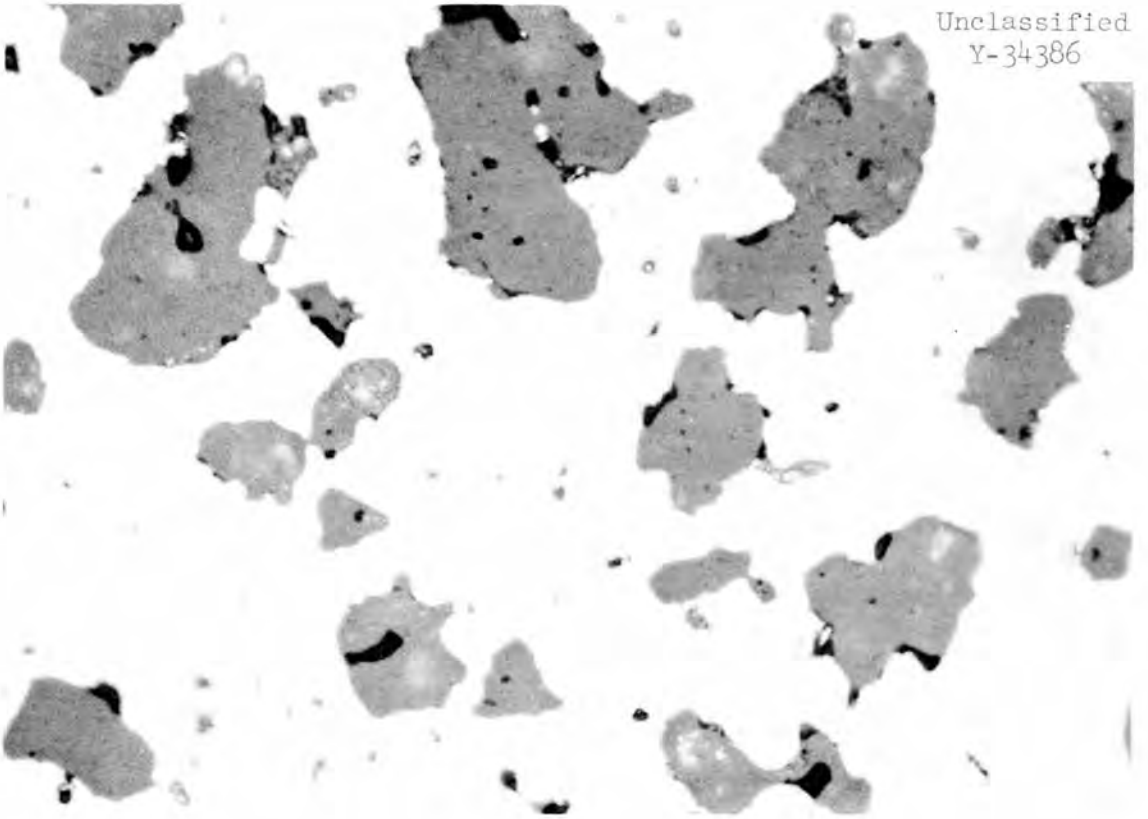

Figure 14. Microstructure of 30 weight per cent type B-Eu_2O_3 dispersed in nickel and heat treated at 1230°C for one and one-half hours under hydrogen. As polished. 1000X.

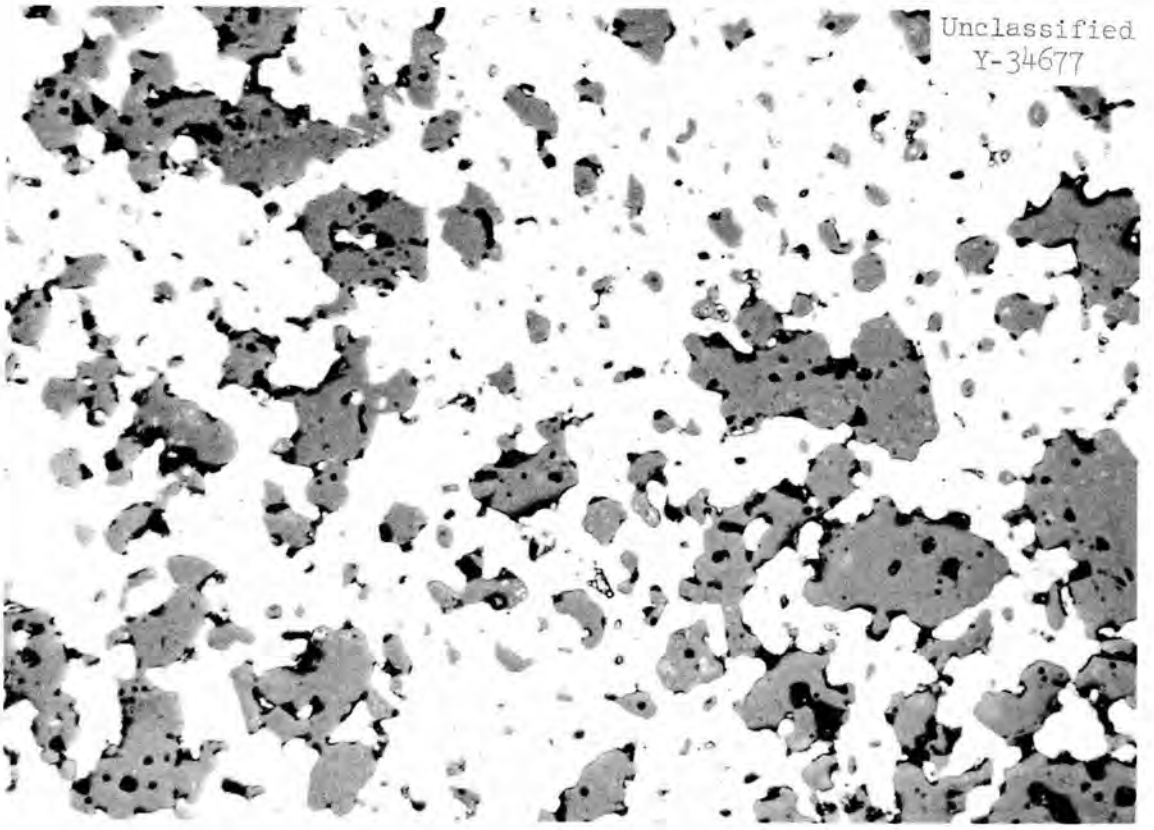

Figure 15. Microstructure of 30 weight per cent type C-Eu_2O_3 dispersed in nickel and heat treated at 1230°C for one and one-half hours under hydrogen. As polished. 500X.

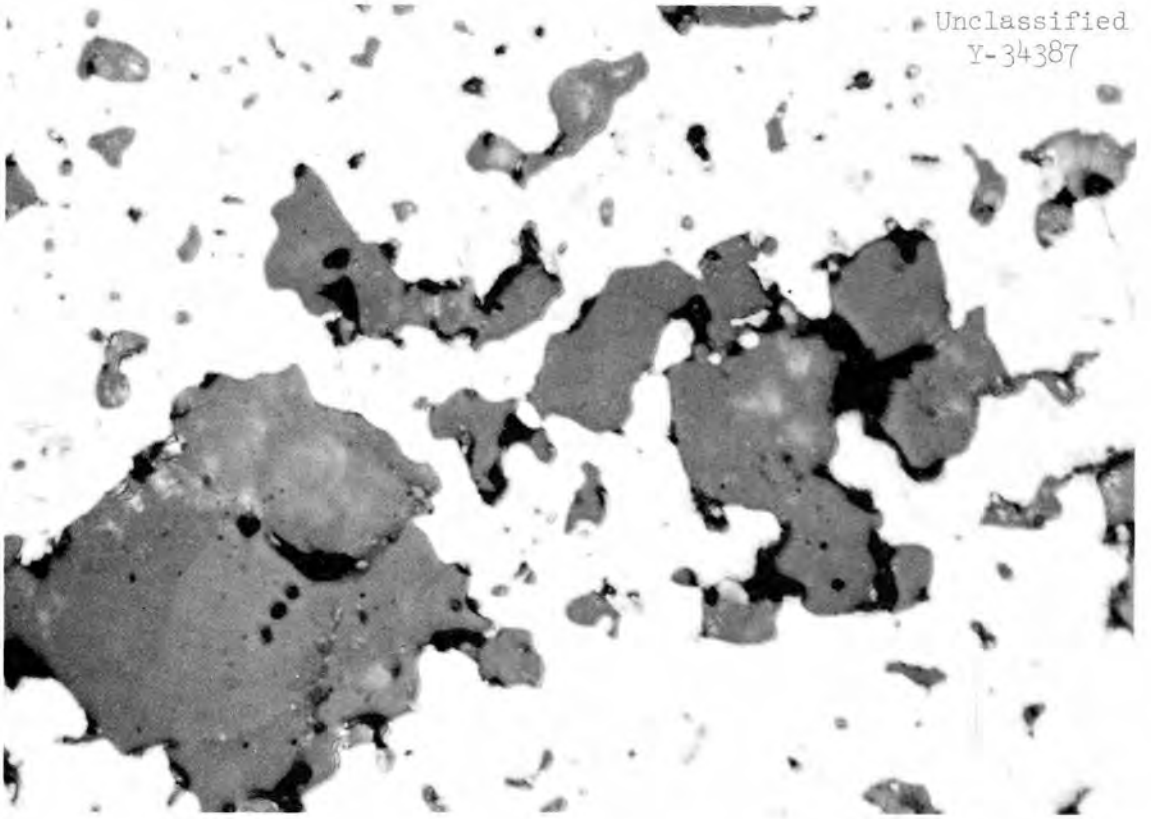

Figure 16. Microstructure of 30 weight per cent type D-Eu_2O_3 dispersed in nickel and heat treated for one and one-half hours at 1230°C under helium. As polished. 1000X.

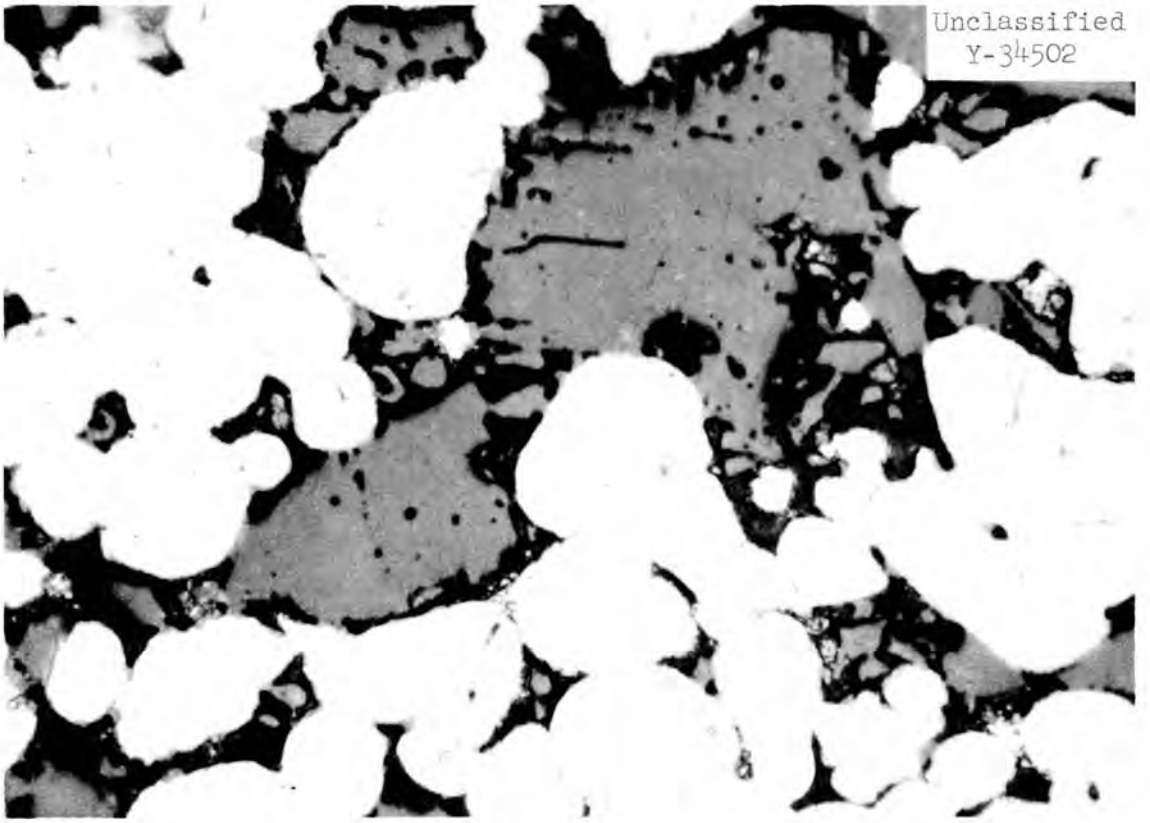

Figure 17. Microstructure of 30 weight per cent type D-Eu_2O_3 dispersed in type 304L stainless steel and heat treated at 1230°C for one and one-half hours under hydrogen. As polished. 1000X.

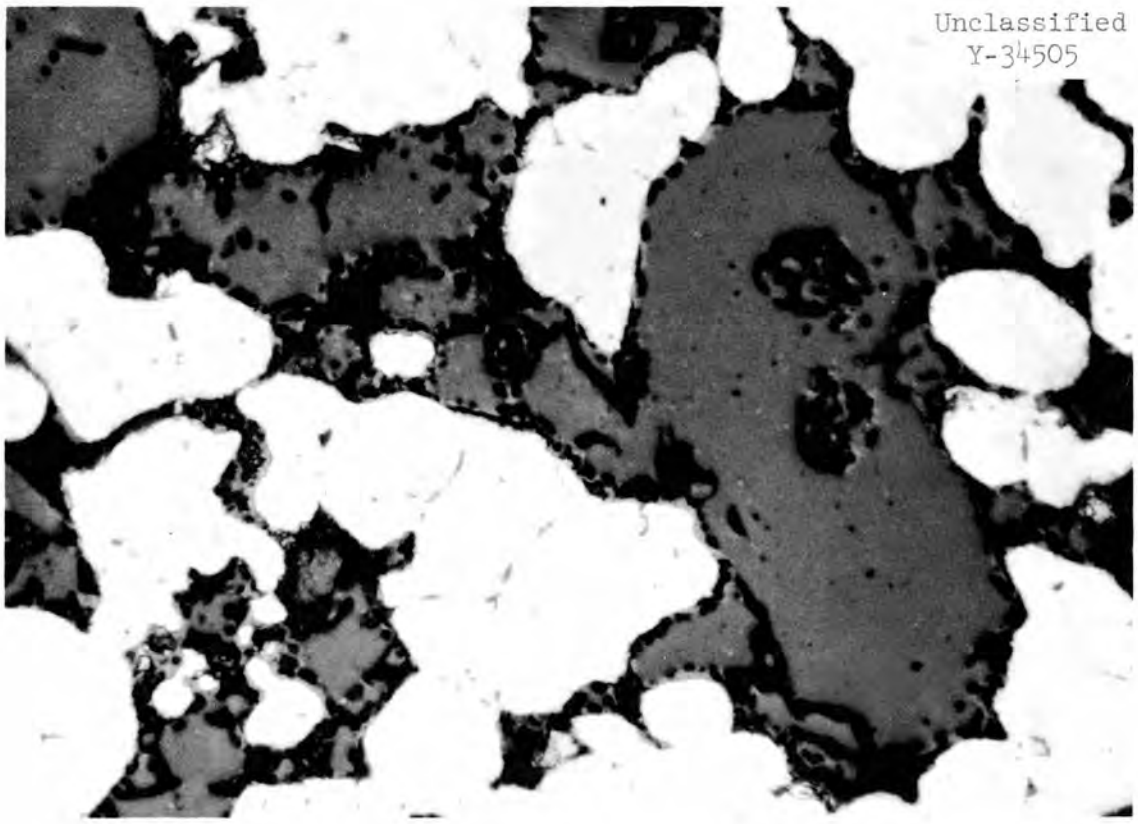

Figure 18. Microstructure of a 30 weight per cent type D-Eu_2O_3 dispersion in type 304L stainless steel heat treated at 1230°C for one and one-half hours under helium. As polished. 1000X.

Although the data have not been reported in the tables, various compacts were also heat treated in vacuum. In general, considerable difficulties were encountered in obtaining reproducible data or results which were comparable to the hydrogen or helium tests. Independent of the original silicon content of the base material, the vacuum heat-treated specimens were covered with a yellow-green film. This film appeared identical with the film observed on reacted compacts heat treated in either a helium or hydrogen atmosphere. It appeared, therefore, that the difficulty could be attributed to the reaction of the compact with the quartz muffle at the elevated heat-treating temperatures. By completely encapsulating the specimens in molybdenum foil the condition was improved; however, it was not completely eliminated. As a result, the vacuum heat-treating data were excluded except for two tests which will be discussed later.

The effect of heat-treating temperature and time on the compatibility of Eu_2O_3 in various dispersants is shown in Table X. Compacts containing type D-Eu_2O_3 dispersed in various matrices were heat treated under a hydrogen or helium atmosphere for times ranging from one to sixteen hours at temperatures of 900–1250°C. Only the type D-Eu_2O_3 was used in these tests since similar results were expected from the various other type oxides.

Examination of the data presented in Table X indicated that the compact volume change increased with both increasing heat-treatment time and temperature. A fairly consistent decrease in compact weight can also be noted as the heat-treating temperature and time are increased. This trend appeared independent of the heat-treating

TABLE X

EFFECT OF TEMPERATURE AND TIME ON THE COMPATIBILITY OF Eu_2O_3 IN VARIOUS DISPERSANTS

Matrix Material	Temp. (°C)	Time (hr)	Atmosphere	Weight Change (g)	Volume Change (%)	Remarks
Stainless Steel-Type 304B*	900	1	H_2	-0.0045	+ 1.13	Specimen appeared metallic
	1000	1	H_2	-0.0060	+ 2.18	Specimen appeared tarnished
	1100	1	H_2	-0.0055	+ 4.34	Specimen covered with yellow-green film
	1175	1	H_2	-0.0080	+ 5.81	Specimen covered with yellow-green film
	1230	1	H_2	-0.0075	+ 6.39	Specimen covered with yellow-green film
Stainless Steel-Type 347B	1230	$1\frac{1}{2}$	H_2	-0.0073	+ 3.53	Specimen covered with yellow-green film
	1230	4	H_2	-0.0118	+ 5.25	Specimen covered with yellow-green film
	1230	16	H_2	-0.0137	+ 7.12	Specimen covered with yellow-green film
	1230	$1\frac{1}{2}$	He	-0.0054	+ 2.95	Specimen covered with yellow-green film
	1230	4	He	-0.0102	+ 5.32	Specimen covered with yellow-green film
	1230	$1\frac{1}{2}$	Vac	-0.0062	+ 3.34	Specimen covered with yellow-green film
	1230	4	Vac	-0.0108	+ 4.78	Specimen covered with yellow-green film

TABLE X (continued)

Matrix Material	Temp. (°C)	Time (hr)	Atmos-phere	Weight Change (g)	Volume Change (%)	Remarks
Stainless Steel-Type 304L	1200	$1\frac{1}{2}$	H_2	-0.0033	- 1.14	Specimen only slightly covered with film
	1230	$1\frac{1}{2}$	H_2	-0.0051	- 4.22	Specimen only slightly covered with film
	1230	16	H_2	-0.0097	- 5.15	Specimen only slightly covered with film
	1230	$1\frac{1}{2}$	He	-0.0034	- 1.50	Specimen only slightly covered with film
Type III-Chromium	1200	$1\frac{1}{2}$	H_2	-0.0036	- 3.67	Specimen only slightly covered with film
	1230	$1\frac{1}{2}$	H_2	-0.0036	- 4.97	Specimen only slightly covered with film

*Specimens initially cold pressed at 10 tsi pressure.

atmosphere, for at equivalent heating temperatures and times the weight loss was approximately constant in helium, hydrogen, and vacuum. The gross volume differences noted previously between the hydrogen and helium heat-treated type 347B stainless steel-base dispersions were not observed in these data.

Metallographic examination of the sixteen-hour heat-treated type 347B stainless steel-base compact revealed that practically all of the Eu_2O_3 had reacted with the steel, resulting in a substantially thicker film formation around the steel particles than previously reported in the shorter time tests. This phenomenon is illustrated in Figure 19. It was interesting to note that the Eu_2O_3 which remained in the compact was single phase. No indication of the red colored soluble phase previously reported to be a result of reaction was observed in the specimen. It thus appeared that the red phase, which composed nearly the entire microstructure of the Eu_2O_3 in the one and one-half hour heat treatments, vaporized during the longer heat treatments. Attempts were made again to mechanically extract the reaction product surrounding the steel particles but, although it had increased in thickness, it was still too narrow to remove by microchiseling.

The microstructure of a type 304L stainless steel-base compact heat treated at 1230°C for sixteen hours under hydrogen is shown in Figure 20. Little differences were noted between this microstructure and that shown in Figure 17, page 57. The thin reaction layer shown in Figure 17 between the Eu_2O_3 and steel particles is absent in Figure 20, as well as the small deposits noted in various regions on the periphery of the steel particles.

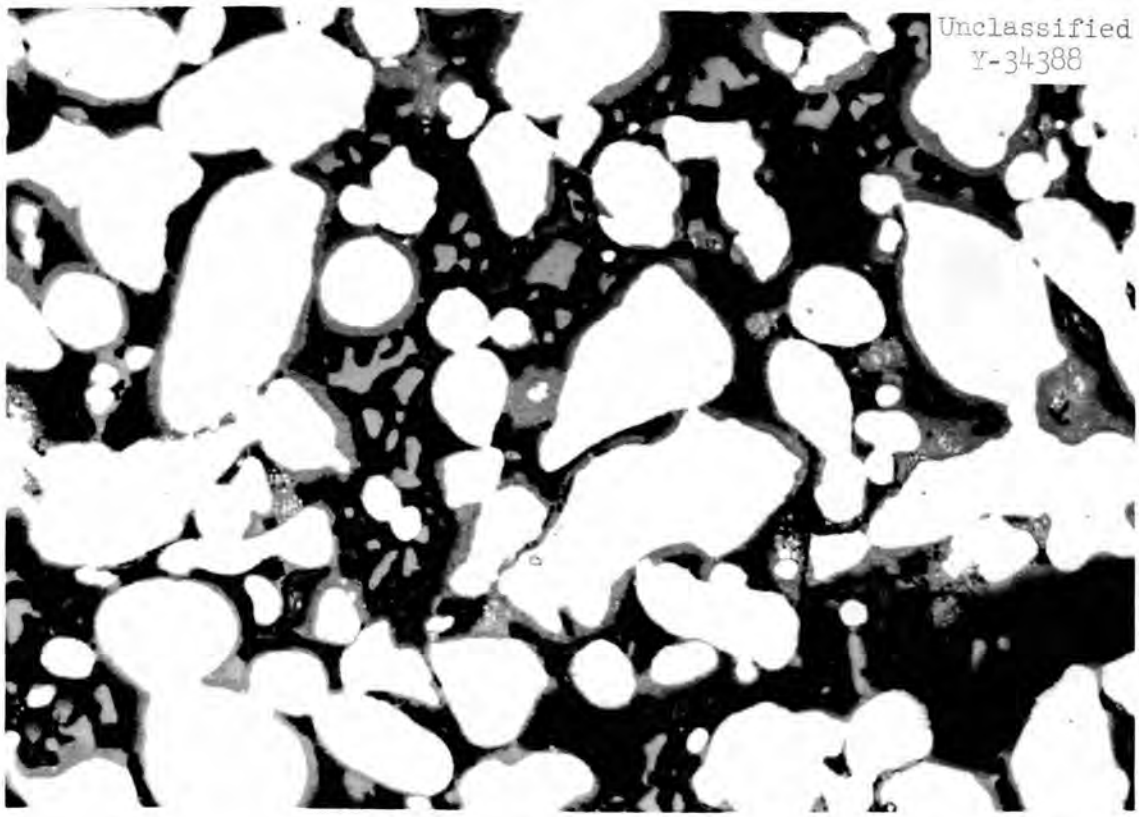

Figure 19. Microstructure of a 30 weight per cent type D-Eu_2O_3 dispersion in type 347B stainless steel heat treated at 1230°C for 16 hours under hydrogen. As polished. 500X.

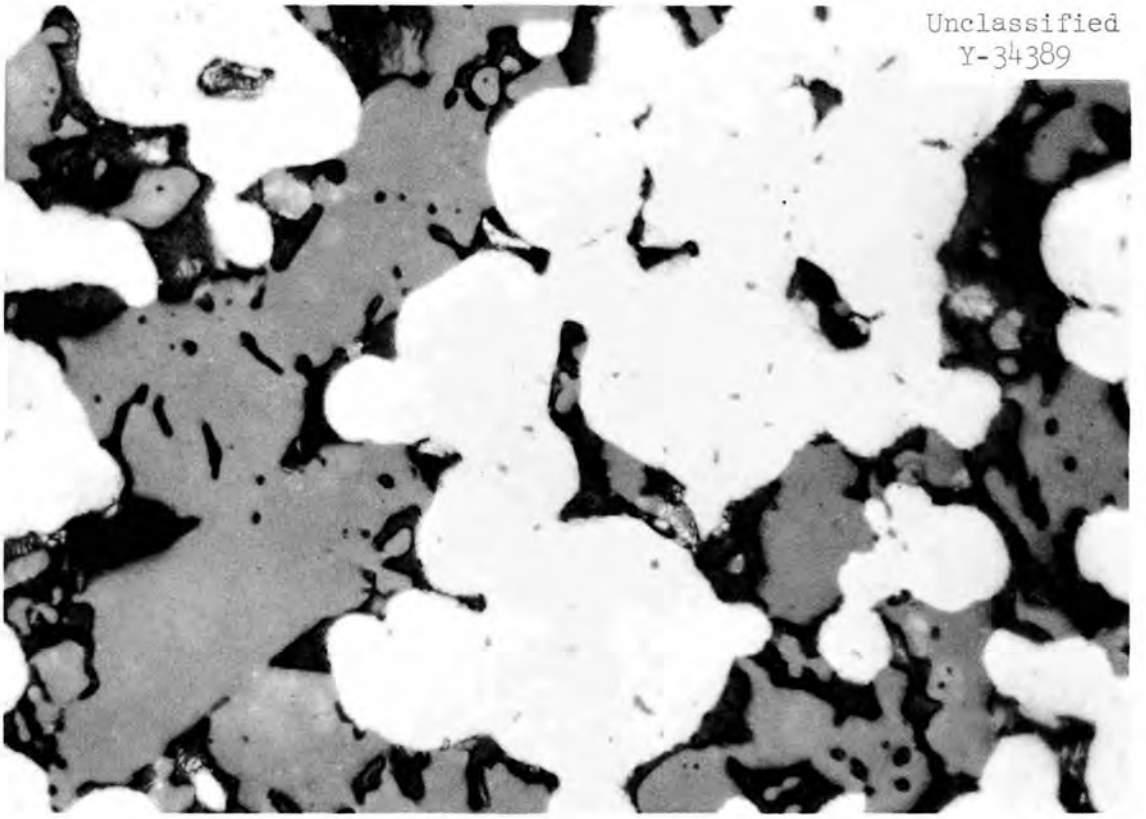

Figure 20. Microstructure of 30 weight per cent type D-Eu_2O_3 dispersed in type 304L stainless steel and heat treated 16 hours at 1230°C under hydrogen. As polished. 1000X.

Considerably more sintering of the type 304L stainless steel particles can be observed in this longer heat-treated compact.

Thus, it appeared that the stability of Eu_2O_3 in the various dispersants was a function of silicon content and heat-treating time and temperature. As a result of these observations silicon-base compacts were heat treated to verify the experimental data and possibly establish a reaction mechanism. Compacts containing Eu_2O_3 and SiO_2 mixtures were also heat treated since in certain instances the oxygen content of the matrix seemed to play an important role in the degree of reaction. The results of the heat treatment of these compacts at 1200°C for one and one-half hours are summarized in Table XI. A considerable spread in the volume and weight change data for the silicon-base compacts can be noted. It appeared that the compacts which had the larger volume increases possessed weight gains while small volume changes induced weight losses. It should be noted that it is between the two die size variations where the sharp distinctions in the data exist. More consistent volume change data were noted in the SiO_2-base dispersions. In all cases, the volume changes noted in SiO_2-base dispersions were larger than the changes in the silicon-base compacts. The weight changes were also generally greater and more consistent in these compacts.

Similarly, anomalies were also observed in the film formation on the silicon-base compacts. Only the compacts which had relatively large volume increases were coated with a yellow-green film. The remaining silicon-base compacts appeared tarnished and completely void

TABLE XI

EFFECTS OF HEAT TREATMENT ON Eu_2O_3-BEARING SILICON AND Eu_2O_3-BEARING SiO_2 DISPERSIONS

Matrix Material	Compacting Die Size (in.)	Weight Change (g)	Volume Change (%)	Remarks
Silicon	5/16	+0.0025	+ 4.66	Specimen covered with yellow-green film
	5/16	+0.0014	+ 1.77	Specimen covered with yellow-green film
	5/16	+0.0012	+ 2.0	Specimen covered with yellow-green film
	5/16	+0.0011	+ 2.0	Specimen covered with yellow-green film
	1/4	-0.0146	- 0.31	Specimen appeared tarnished, film noted in boat
	1/4	-0.0051	+ 0.83	Specimen appeared tarnished, film noted in boat
	1/4	-0.0046	+ 0.57	Specimen appeared tarnished, film noted in boat
SiO_2	1/4	-0.0162	+ 8.76	Specimen covered with yellow-green film
	1/4	-0.0135	+ 9.23	Specimen covered with yellow-green film
	1/4	-0.0155	+ 7.88	Specimen covered with yellow-green film

Type D-Eu_2O_3 dispersed in all compacts.

of the film. The yellow-green film, however, was present on portions of the molybdenum boats used to contain these specimens during heat treatment.

Metallographic examination of the silicon-base dispersions indicated that essentially all of the Eu_2O_3 had reacted with the silicon. The resultant microstructure can be seen in Figure 21. The presence of the reaction product and an isolated unreacted Eu_2O_3 particle is apparent. Unlike the reaction products noted in the steel-base dispersions, this product appeared quite metallic and closely resembled the appearance of an intermetallic phase. Attempts to metallographically examine the SiO_2-base dispersions were unsuccessful due to the complete lack of compact strength.

Postulating that silicon was directly associated with the instability of Eu_2O_3 in commercial steels, attempts were made to prepare possible standards so that by comparison the various observed by-products of the reaction could be identified. Since the formation of a silicide appeared likely, various europium-silicon alloys were prepared and examined by both metallography and x-ray diffraction to establish standards for the various silicides. The results of these studies on the cast alloys are summarized in Table XII. It was observed in arc melting these alloys that considerable vaporization of the europium metal had occurred. This vaporization accounted for the decrease in europium content of the cast alloys.

Employing x-ray diffraction and metallographic techniques, the basic microstructures of the cast alloys containing 9.35–63.9 weight per cent europium were established. The microstructure as shown in

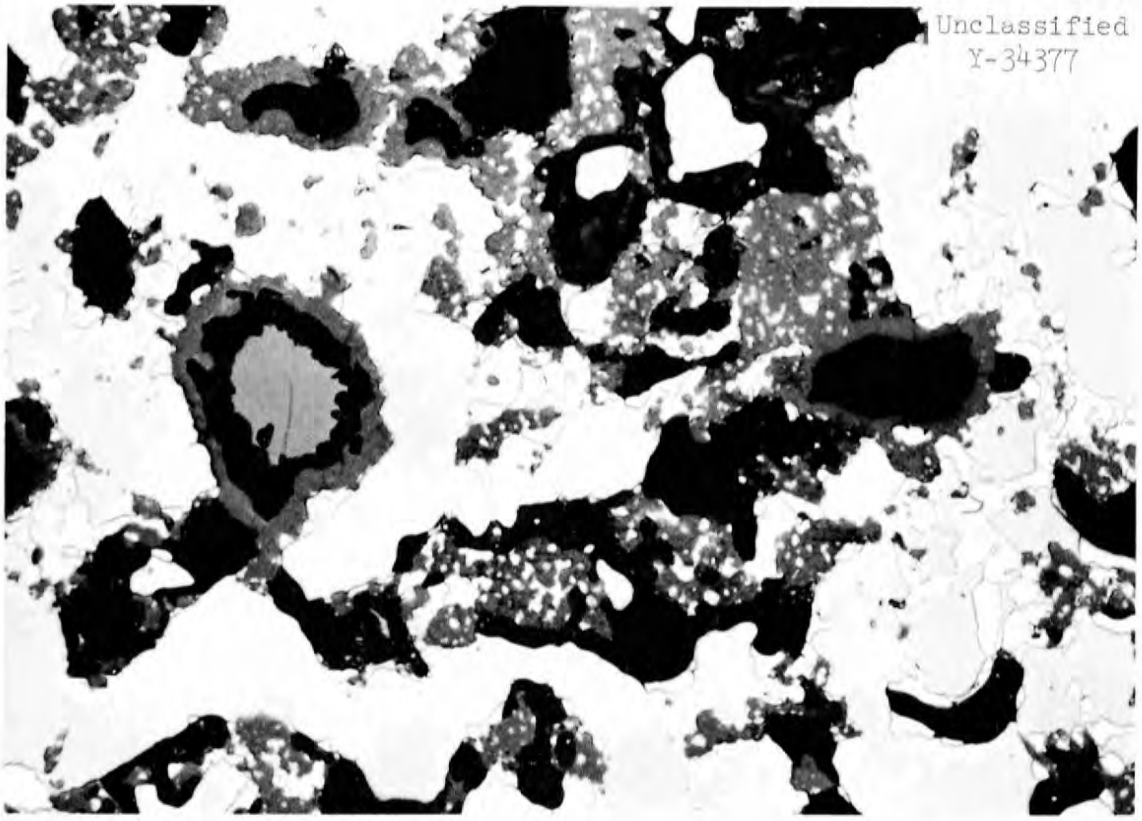

Figure 21. Microstructure of 30 volume per cent type D-Eu_2O_3 dispersed in silicon and heat treated at 1200°C for one and one-half hours under hydrogen. As polished. 500X.

TABLE XII

SUMMARY OF RESULTS ON VARIOUS CAST EUROPIUM-SILICON ALLOYS

Alloy Number	Europium (at %)	Charged (wt %)	Europium Recovered (wt %)	Relative Cast Microstructure
1	3	14.34	9.35	Silicon + $EuSi_2$
2	6	25.67	22.41	Silicon + $EuSi_2$
3	10	37.55	33.05	Silicon + $EuSi_2$
4	20	57.50	54.26	Silicon + $EuSi_2$
5	30	69.84	63.90	Silicon + $EuSi_2$
6	40	78.30	73.73	$EuSi_2$ + unknown phase
7	50	84.40	77.60	Possibly $EuSi_2$+ unknown phase
8	60	89.03	84.88	Possibly two unknown phases
9	70	92.66	86.02	Europium + unknown phase
10	80	95.58	89.28	Europium + unknown phase
11	90	97.99	91.02	Europium + unknown phase

Alloy charged weight totaled 50 grams.

Table XII consisted of silicon and $EuSi_2$. The diffraction pattern obtained on the silicide corresponded extremely well with data given by Perri et al. (10), for $EuSi_2$; namely, a body-center tetragonal cell with a = 4.29 Å and c = 13.66 Å. Two other distinct silicides seemed present in the system, neither of which was positively indexed. Europium metal was observed in the cast microstructure of alloys numbers 9, 10, and 11. Examination of the silicon diffraction lines in the various alloys indicated that the solubility of europium in silicon was small for no lattice parameter changes were noted.

The microstructure of the 22.4 weight per cent europium-silicon alloy is shown under bright-field illumination and polarized light in Figure 22(a) and (b), respectively. The silicon appears as the isotropic phase, whereas, the $EuSi_2$ exhibits anisotropic properties under polarized light. The relative amount of the $EuSi_2$ was found to increase in the microstructure of alloys numbers 1–5 as the percentage of europium increased. The microstructure of the 73.7 weight per cent europium-silicon alloy is also shown under bright field and polarized light in Figure 23(a) and (b), respectively. A comparison of the two figures indicates that both phases possess anisotropic properties. The existence of $EuSi_2$ in this microstructure was established by x-ray diffraction. Careful examination of the microstructure of the 84.88 weight per cent europium-silicon alloy under bright field and polarized light, which are shown in Figure 24(a) and (b), respectively, indicated that all of the phases were not anisotropic. The light phase in Figure 24(a) appears to be isotropic under polarized light.

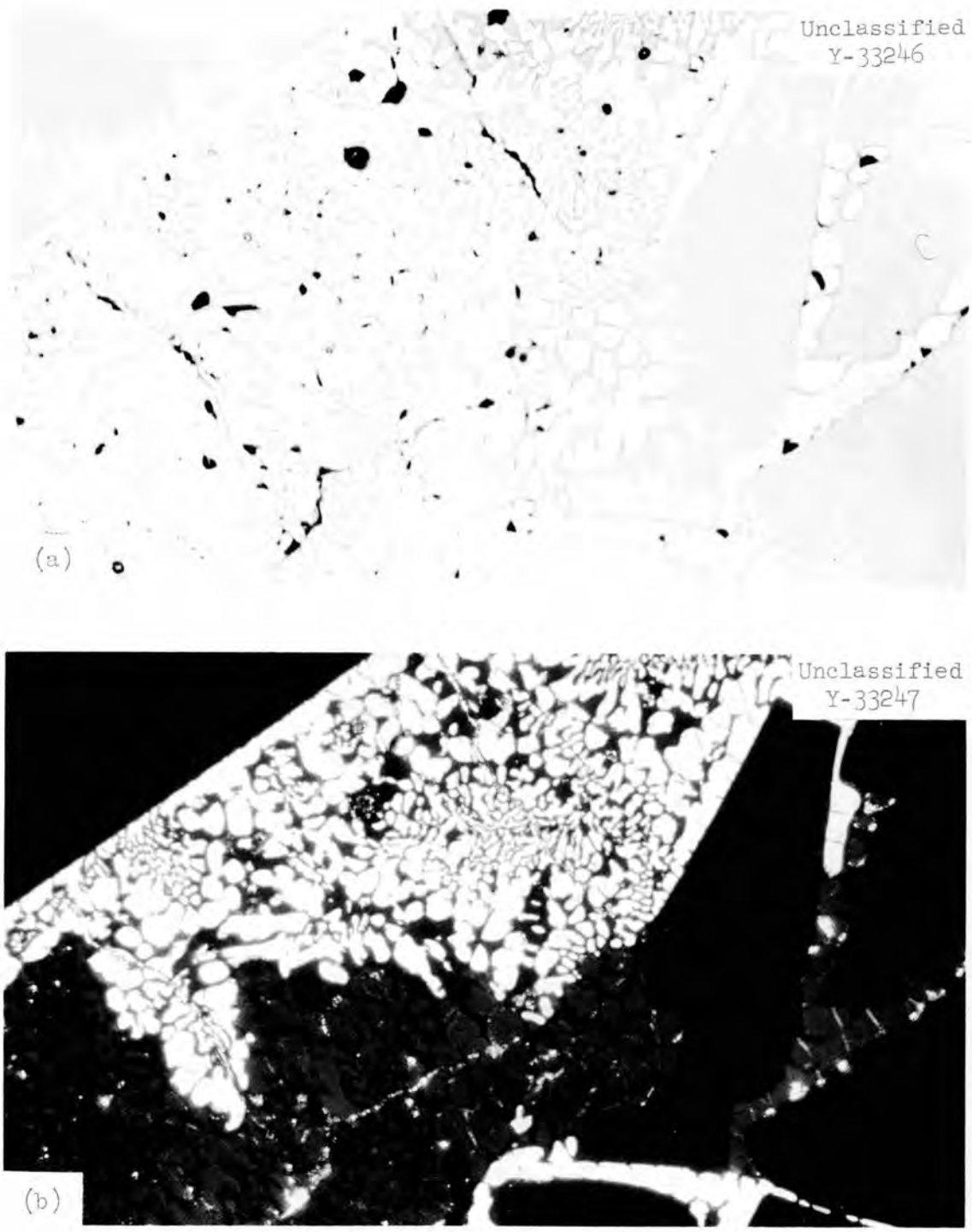

Figure 22. Microstructure of the cast 22.4 weight per cent europium-silicon alloy under (a) bright field and (b) polarized light. As polished. 500X.

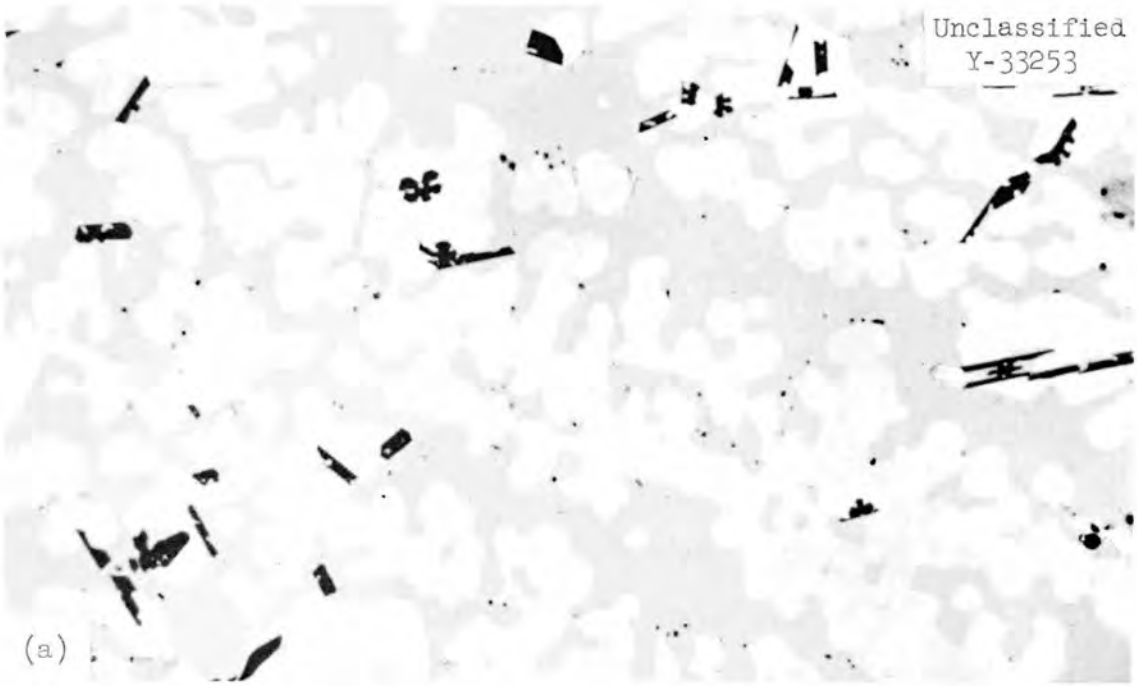

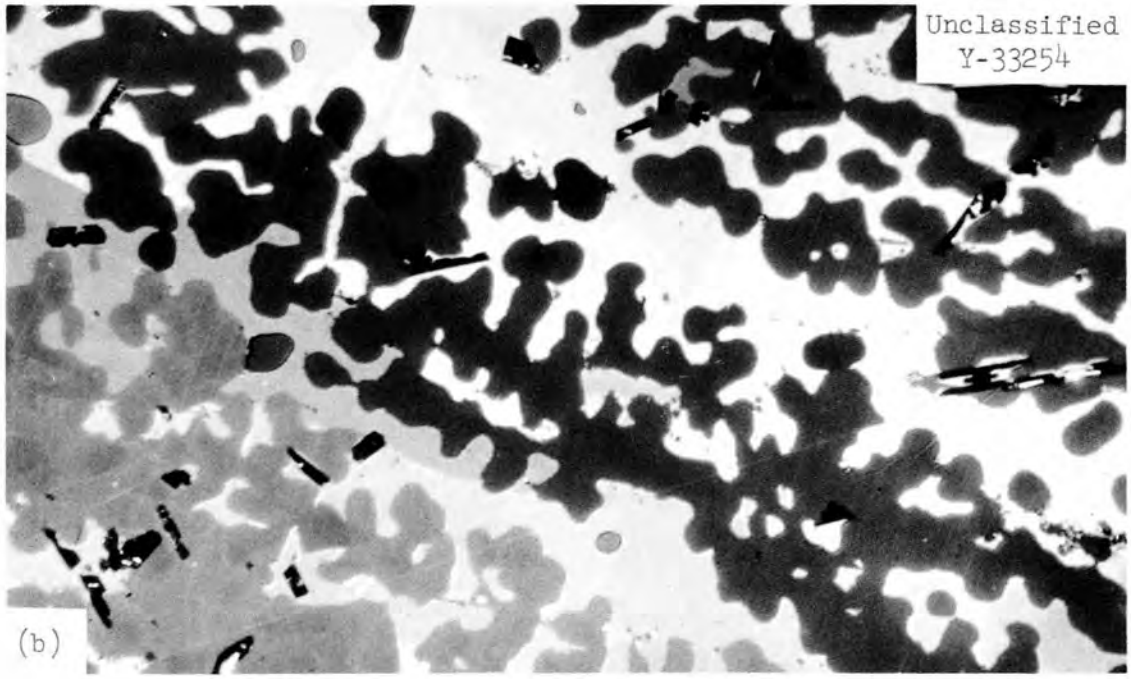

Figure 23. Microstructure of the cast 73.7 weight per cent europium-silicon alloy under (a) bright field and (b) polarized light. As polished. 500X.

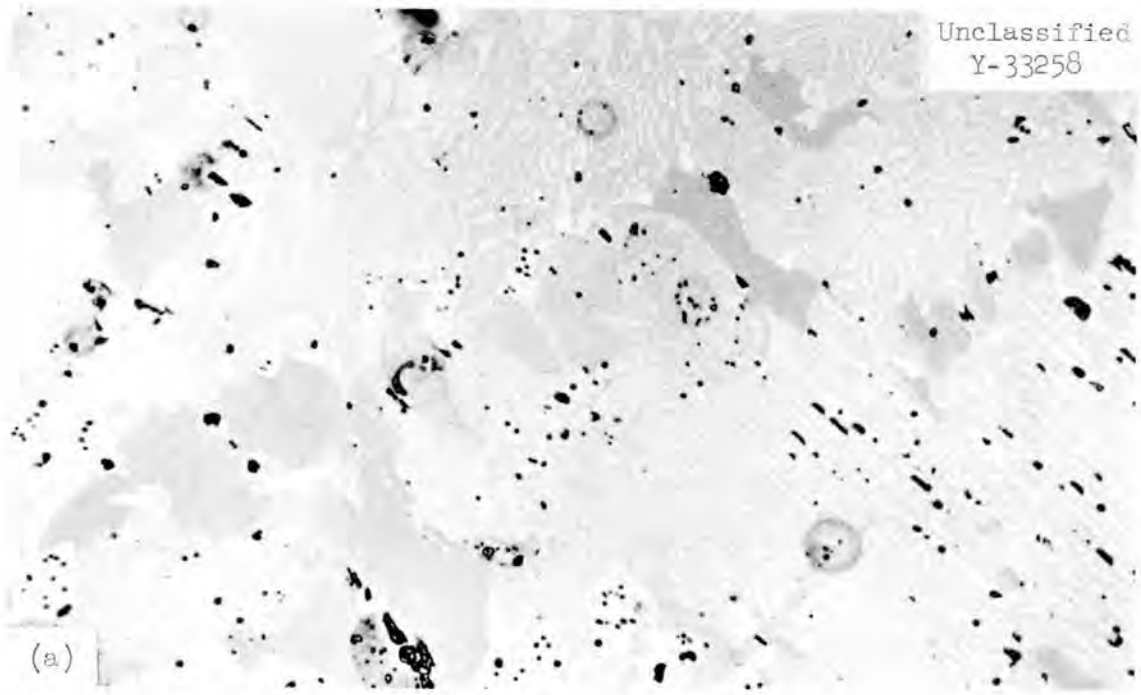

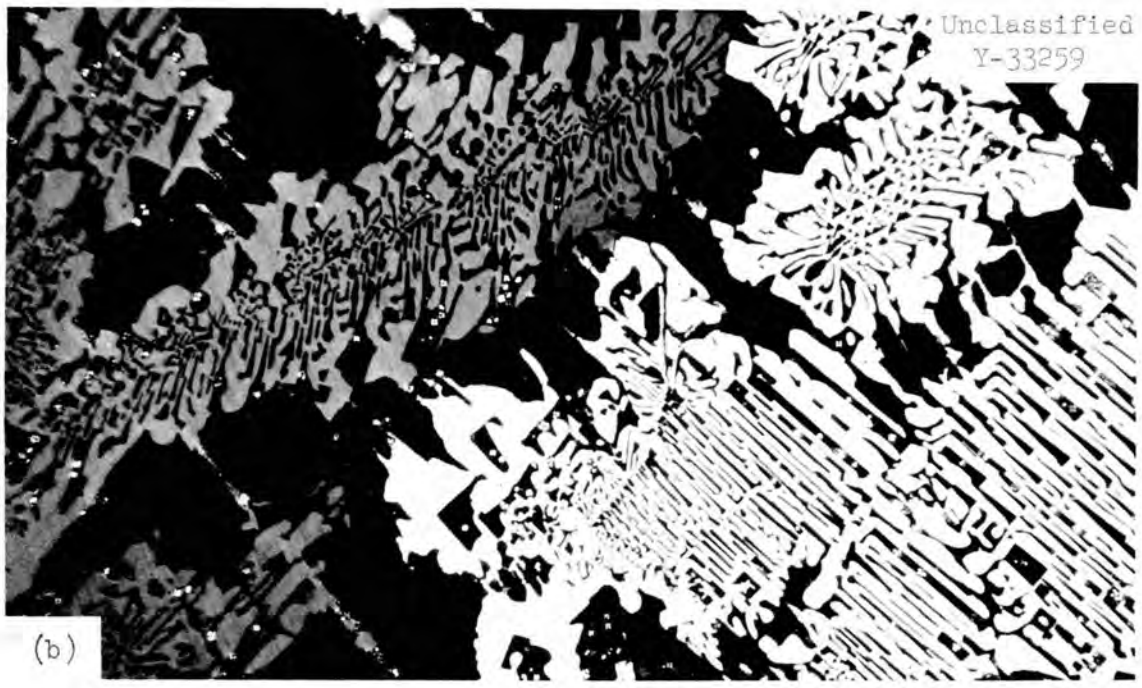

Figure 24. Microstructure of the cast 84.88 weight per cent europium-silicon alloy under (a) bright field and (b) polarized light. As polished. 500X.

Several of the europium-silicon alloys were also heat treated to improve homogeneity and evaluate the effect of heat treatment on the cast structure. Heat treating alloys numbers 1, 3, 5, 7, and 9 for 72 hours at 750°C resulted in the further reduction of the europium content and a subsequent interaction of the europium with the quartz capsule. A preliminary examination of these heat-treated specimens showed that no considerable microstructural changes had occurred.

Since the formation of various silicides was established in the europium-silicon alloy system, the metallic-appearing phase which was previously observed as a reaction product in heat-treated Eu_2O_3-silicon compacts was further investigated. By employing a microchisel, it was possible to concentrate this phase to the extent that a powder x-ray diffraction pattern could be obtained. Examination of this pattern showed that the diffraction lines were identical to those of $EuSi_2$ obtained in the experimental alloys. As previously mentioned, it was not possible to concentrate the reaction products noted in the silicon-bearing stainless steel-base dispersions. The various x-ray patterns obtained on filings from these compacts failed to indicate the presence of the $EuSi_2$. The high concentration of steel and Eu_2O_3 in these compacts completely overshadowed any possible silicide lines. Likewise, the efforts to extract and identify the various films observed in the other base dispersants were unsuccessful due to their small concentrations and deposit thinness.

The yellow-green appearing film which was observed to coat the specimens and heat-treating boats when a reaction occurred was examined spectrographically. Powder specimens also were taken for x-ray

diffraction. The spectrographic analyses on the films extracted from three different compacts are shown in Table XIII. A particularly strong europium content was noted in each sample. No differences were observed between the analyses of the three films. The x-ray analyses failed to establish the identity of the film in terms of known x-ray data. The x-ray data reported for the cubic EuO and EuN did not correspond to these diffraction data. However, due to the uncertainty of any reliable information on europium oxides other than Eu_2O_3, the present data do not eliminate other europium oxides. The diffraction lines could be interpreted to indicate the presence of europium metal; however, numerous unindexed lines remained in the patterns.

Since it was essentially impossible to identify the various reaction products observed in these studies, the deduction of a reaction mechanism from the data is therefore quite difficult. The role of silicon in the reaction of Eu_2O_3 with the stainless steel was established although the form by which silicon entered into the reaction was questionable. It was established that silicon in either elemental or in oxide form reacts with Eu_2O_3 resulting in the formation of a silicide or silicate, respectively. The ability of silicon to reduce Eu_2O_3 to either a lower valent oxide or the metal would not at first appear to be feasible since the reported standard free energies of formation of the lanthanon oxides are generally greater than that for SiO_2 at the temperatures of interest. Since the actual free energies of formation of the lanthanon oxides are dependent on the testing environment, the actual conditions under which the reactions are occurring must be considered. For example, it would be necessary to

TABLE XIII

SPECTROGRAPHIC ANALYSIS ON REACTION PRODUCT FILMS EXTRACTED FROM DIFFERENT SPECIMENS

Element	Concentration		
	Sample A	Sample B	Sample C
Al			
Cu			
Eu	Very strong	Very strong	Very strong
Fe	Trace		Trace
Mo	Weak	Weak	Weak
Ni			
Si	Weak	Weak	Weak
W			

take into account the existing partial pressures of water, hydrogen, and oxygen and the high vapor pressure of europium and/or EuO.

Since the formation of the europium-bearing film was noted on both the specimen and heating boat in almost every reacted compact, the possible vaporization of the reduced Eu_2O_3 constituent was suggested; namely, europium metal or a lower valent europium oxide. The volatility of these constituents would then account for the increased compact weight loss with increasing heat-treatment time and temperature. To better establish the composition of the reduced constituent a total oxygen analysis was performed on compacts containing type D-Eu_2O_3 dispersed in type 347B stainless steel and heat treated at 1230°C for varying times. Prior to considering the data on the reacted compacts, the effect of heat treating the individual materials under hydrogen at 1230°C was studied. These data along with the oxygen content of the reacted compacts as a function of time and heat-treating atmosphere are summarized in Table XIV. It can be seen in Table XIV that both base constituents lost oxygen upon being treated while the oxygen content of the reacted compacts remained essentially constant. Again a consistent decrease in compact weight can be observed as a function of increasing time. The essentially constant oxygen analyses in the heat-treated samples tend to suggest that elemental europium is formed in the reduction of Eu_2O_3 and subsequently vaporized from the compact. The slight increase in oxygen content with time, if real, might be explained by the reaction of the vaporized europium with the oxygen and water vapor in the furnace atmosphere. Under these conditions the resulting europium compound should be a hydrated oxide. It was interesting to

TABLE XIV

THE OXYGEN CONTENT OF HEAT-TREATED THIRTY WEIGHT PER CENT TYPE D-Eu_2O_3-347B STAINLESS STEEL COMPACTS AS A FUNCTION OF HEATING TIME AND ATMOSPHERE

Compact* Constituents	Heating Time (hr)	Heating Atmos-phere	Weight Change (g)	Volume Change (%)	Oxygen** Content (wt %)
Type 347B Stainless Steel	0				0.17
Type D-Eu_2O_3	0				13.80
Type 347B Stainless Steel	$1\frac{1}{2}$	H_2	-0.0056	-17.13	0.0085
Type D-Eu_2O_3	$1\frac{1}{2}$	H_2	-0.0083	- 2.81	13.65
Type D-Eu_2O_3-347B Stainless Steel	$1\frac{1}{2}$	H_2	-0.0071	+ 3.53	4.12
	4	H_2	-0.0107	+ 5.09	4.37
	16	H_2	-0.0192	+ 6.54	4.58
	$1\frac{1}{2}$	He	-0.0053	+ 2.95	3.03
	4	He	-0.0102	+ 5.32	3.57
	$1\frac{1}{2}$	Vac	-0.0060	+ 3.34	3.12
	4	Vac	-0.0107	+ 4.62	3.62

*Compacts were prepared by cold pressing at 33 tsi pressure and weighed initially about 1.5 grams. Heat-treating temperature: 1230°C.

**Oxygen content of each compact is the average of three separate determinations. Accuracy of oxygen analysis ± 5 weight per cent.

note in a subsequent experiment that the interaction of europium metal with distilled water formed a yellow-green appearing compound which upon removal and exposure to air slowly converted to the characteristic white oxide. The yellow-green film, however, noted on the reacted samples did not change in color on exposure to air. A further observation may be pertinent to the conditions under which this film forms. The yellow-green film was also observed on the inner surfaces of the arc-melting furnace when upon completion of an arc melt the furnace interior was exposed to air.

Thus the mechanism by which silicon and/or SiO_2 could enter into reaction with Eu_2O_3 in the commercial steels is postulated by the following series of equations:

$$2\ Eu_2O_3 + 5\ Si \rightarrow 3\ Eu\uparrow + EuSi_2 + 3\ SiO_2 \tag{1}$$

$$Eu_2O_3 + SiO_2 \rightarrow Eu\uparrow + EuSiO_x \tag{2}$$

$$Eu(s) \rightleftarrows Eu(v) \tag{3}$$

$$2\ Eu(s) + O_2 + x\ H_2O \rightarrow 2\ EuO \cdot x\ H_2O \tag{4}$$

The reactions as stated in equations 1 and 2 are simplified versions of chemical reactions which involve several complex stages. As stated, the resulting reaction products would, therefore, be either the europium disilicide and/or the silicate and a hydrated europium oxide. Silicon dioxide would be present with the silicon reaction products to serve as an oxygen balance. The particular temperature and atmosphere in which the europium reacted with the tramp water vapor and oxygen could have stabilized the resulting yellow-green compound from further change on exposure to air.

As previously stated, the interaction of the various metallic oxides with Eu_2O_3 was observed by several investigators. Such

interactions, however, were not considered to be major contributors since the total amount of the metallic oxide was so limited. Had similar experiments been conducted in an oxygen-rich atmosphere considerable differences in the compact reaction products would have been expected.

In concluding this discussion, it may be mentioned that the greatest obstacle in evaluating the experimental data was the absence of fundamental physical and chemical information on europium and its compounds as well as their various basic thermodynamic properties. When such information is obtained, a more detailed investigation and verification of the proposed reaction mechanism should be conducted. Such an investigation was beyond the scope of the aforedescribed study.

CHAPTER VII

CONCLUSIONS

The following conclusions can be stated as a result of the reported investigation.

1. Europium oxide reacted with commercial stainless steel at temperatures above 1000°C as a function of silicon content. Compacts utilizing stainless steel powders containing approximately two weight per cent silicon increased about six per cent in volume while the volume of similar compacts containing stainless steel with 0.11 per cent silicon decreased. The deposition of an europium-bearing yellow-green film was noted on all of the stainless steel-base dispersions and was considered a product of reaction. Along with this film formation, a reaction product was also noted in the Eu_2O_3 particles in the high silicon-bearing stainless steel-base compacts. This product was found extremely soluble in water. The formation of this reaction product, however, was not observed in the Eu_2O_3 particles in the type 304L stainless steel-base dispersions.

2. Europium oxide was stable in dispersants containing essentially no silicon. Slight interactions between Eu_2O_3 and chromium oxide were noted and in particular where the chromium had a relatively high oxygen content. The reaction noted in the type II-chromium-base dispersions was not accompanied by the appearance of a reaction product in the Eu_2O_3 particles. The absence of this reaction product was not understood.

3. The various conditioning treatments for the Eu_2O_3 employed in these studies appeared to have no affect on the stability of the oxide in the various dispersants.

4. The presence of the reaction in the high silicon-bearing stainless steel-base dispersions was essentially independent of the hydrogen, helium, and vacuum heat-treating atmospheres. The degree of reaction, however, was greater in the hydrogen atmosphere.

5. Heat-treating temperature and time had an effect on the degree of reaction in the high silicon-bearing stainless steel-base dispersions containing Eu_2O_3. The degree of reaction increased as the heating time and temperature was increased. The compact weight loss was generally observed to increase with increasing time at temperature.

6. The reaction of Eu_2O_3 with silicon and SiO_2 produced, in general, compact volume increases and the deposition of the europium-bearing film. Certain unexplained anomalies, however, were noted in the silicon-base dispersions. The formation of $EuSi_2$ was established as a reaction product in the silicon-base compacts.

7. Preliminary evaluation of the various europium-silicon alloys ranging from approximately 9 to 91 weight per cent europium indicated the possible existence of at least three silicides. The microstructures of cast alloys ranging from 9 to 63 weight per cent europium consisted of silicon and $EuSi_2$. Considerable amounts of europium were lost in each alloy during arc melting as a result of vaporization.

8. The basic reaction products noted in the stainless steel-base compacts were not positively identified, mainly because of insufficient quantities of reacted material for examination and the lack of essential standards. Therefore, it was possible only to postulate a reaction mechanism.

LIST OF REFERENCES

1. Leitten, Jr., C. F., "Development of Eu_2O_3 Dispersions in Iron-Base Materials," Metallurgy Division Annual Progress Report for Period Ending October 10, 1957, ORNL-2422, 136–38.

2. Ray, W. E. and Beck, C. J., "A Method of Hot Coextruding Complex Shapes Through Round Dies," Nuclear Science and Engineering, 4:481–94, September, 1958.

3. Anderson, W. K. and Dunning, D. N., "Radiation Damage Resistance of Some Rare Earth Cermets," Nuclear Science and Engineering, 4:458–66, September, 1958.

4. Leitten, Jr., C. F., Beaver, R. J. and Cunningham, J. E., Specifications and Fabrication Procedures on Europium-Bearing Absorber Rods for Reactivity Control in Core II of SM-1, ORNL-2733, July 29, 1959.

5. Geller, S. and Wood, E. A., "Crystallographic Studies of Perovskite-Like Compounds, I. Rare Earth Orthoferrites and $YFeO_3$, $YAlO_3$," Acta Crystallographica, 9:563, 1956.

6. Wold, A., Post, B. and Banks, E., "Rare Earth Nickel Oxides," Journal of the American Chemical Society, 79:4911, 1957.

7. Jonker, G. H. and Van Santen, J. H., "Ferromagnetic Compounds of Manganese with Perovskite Structure," Physica, 16:337, 1950.

8. Wold, A. and Ward, R., "Perovskite-Type Oxides of Cobalt Chromium and Vanadium with Some Rare Earth Elements," Journal of the American Chemical Society, 76:1029, 1954.

9. Eick, H. A., Boenziger, N. C. and Eyring, L., "Lower Oxides of Sm and Eu Preparation and Crystal Structure of $SmO_{0.4-0.6}$, SmO and EuO," Journal of the American Chemical Society, 78:5147, 1956.

10. Perri, J. A., Binder, J. and Post, B., "Rare Earth Metal Disilicides," Journal of Physical Chemistry, 63:616–19, 1959.

11. DuBose, C. K. H. and Gray, R. J., "Metallographic Preparation of Lanthanon-Bearing Materials." Oak Ridge National Laboratory, 1960. Unpublished material.

ORNL-2946
UC-25 Metallurgy and Ceramics
TID-4500 (15th ed.)

DISTRIBUTION

1. C. E. Center
2. Biology Library
3. Health Physics Library
4. Metallurgy Library
5–6. Central Research Library
7. Reactor Experimental Engineering Library
8. ORNL - Y-12 Technical Library, Document Reference Section
9–13. Laboratory Records
14. Laboratory Records, RC
15. A. M. Weinberg
16. J. A. Swartout
17. C. E. Winters
18. R. A. Charpie
19. L. B. Emlet (K-25)
20. J. P. Murray (Y-12)
21. D. S. Billington
22. A. L. Boch
23. E. G. Bohlmann
24. C. J. Borkowski
25. R. B. Briggs
26. F. L. Culler
27. A. P. Fraas
28. W. R. Grimes
29. A. Hollaender
30. A. S. Householder
31. W. H. Jordan
32. C. P. Keim
33. M. T. Kelley
34. H. Kubota
35. J. A. Lane
36. S. C. Lind
37. R. S. Livingston
38. H. G. MacPherson
39. A. J. Miller
40. E. C. Miller
41. K. Z. Morgan
42. M. L. Nelson
43. D. Phillips
44. H. W. Savage
45. L. D. Schaffer
46. H. E. Seagren
47. E. D. Shipley
48. M. J. Skinner
49. C. O. Smith
50. E. H. Taylor
51. J. C. Wilson
52. J. H. Frye, Jr.
53. W. D. Manly
54. J. E. Cunningham
55. G. M. Adamson, Jr.
56. R. J. Beaver
57. E. S. Bomar, Jr.
58. J. H. Cherubini
59. J. H. Coobs
60. J. H. DeVan
61. L. M. Doney
62. D. A. Douglas
63. J. I. Federer
64. R. J. Gray
65. J. P. Hammond
66. T. Hikido
67–76. M. R. Hill
77. E. E. Hoffman
78. W. J. Kucera
79–128. C. F. Leitten, Jr.
129. T. S. Lundy
130. M. M. Martin

131. R. W. McClung
132. C. J. McHargue
133. P. Patriarca
134. M. L. Picklesimer
135. T. K. Roche
136. G. M. Slaughter
137. R. M. Steele
138. A. Taboada
139. W. C. Thurber
140. J. L. Gregg
141. J. H. Koenig
142. E. E. Stansbury
143. D. K. Stevens
144. C. S. Smith
145. R. Smoluchowski
146. H. A. Wilhelm

EXTERNAL DISTRIBUTION

147. D. E. Baker, GE Hanford
148. Ersel Evans, GE Hanford
149–150. D. F. Cope, Oak Ridge Operations
151. H. M. Roth, Oak Ridge Operations
152–161. Division of Reactor Development, AEC, Washington (Att: Col. D. G. Williams)
162–163. New York Operations Office (Att: Chief, Army Reactors Branch)
164–167. U. S. Army Engineering Research and Development Laboratories, Ft. Belvoir, Va. (Att: Chief, Nuclear Power Field Office)
168–169. Office Chief of Engineers, Washington, D. C. (Att: Chief, Nuclear Power Division)
170–171. District Engineer, Eastern Ocean District, U. S. Army Corps of Engineers, New York, N. Y.
172–173. District Engineer, Alaska District, U. S. Army Corps of Engineers, Anchorage, Alaska
174–177. Alco Products, Inc., Schenectady, New York (Att: K. Kasschau)
178–179. Combustion Engineering, Inc., Idaho Falls, Idaho (Att: W. B. Allred)
180–181. The Martin Company, Baltimore, Maryland (Att: J. F. O'Brien)
182–183. Battelle Memorial Institute, Columbus, Ohio (Att: S. Paprocki)
184–738. Given distribution as shown in TID-4500 (15th ed.) under Metallurgy and Ceramics category (75 copies - OTS)